Nanoparticle-Mediated Immunomodulation as a Therapy in Acute and Chronic Spinal Cord Injury

by

Sarah E. Hocevar

A dissertation submitted in partial fulfillment
of the requirements for the degree of
Doctor of Philosophy
(Neuroscience)
in the University of Michigan
2025

Doctoral Committee:

Professor Emeritus Audrey Seasholtz, Co-Chair
Professor Lonnie Shea, Co-Chair
Professor Cynthia Chestek
Assistant Professor Aaron Morris
Associate Professor Parag Patil

Sarah E. Hocevar

shocev@umich.edu

ORCID iD: 0000-0003-1362-0535

© Sarah E. Hocevar 2025

Dedication

This dissertation is dedicated to my parents, without whom this would not have been possible

Table of Contents

Dedication ii

List of Figures vi

Abstract viii

Chapter 1 Overview of Spinal Cord Injury and Treatments 1

1.1 Significance 1

1.2 Pathology of Spinal Cord Injury 1

1.2.1 Acute Phase 2

1.2.2 Inflammatory response and secondary injury 2

1.2.3 Subacute and Chronic Phases 3

1.3 Clinical Interventions 4

1.4 Experimental Therapies 4

1.4.1 Biomaterials 5

1.4.2 Nanoparticles 6

1.4.3 Epothilones and Microtubule Stabilizers 7

1.5 Models of Spinal Cord Injury 8

1.6 Thesis Overview 9

Chapter 2 Early Nanoparticle Intervention Preserves Motor Function Following Cervical Spinal Cord Injury 11

2.1 Authors 11

2.2 Abstract 11

2.3 Introduction 12

2.4 Methods 14

2.5 Results 18
2.5.1 Nanoparticle administration alters immune infiltration into the spinal cord 18
2.5.2 Immune cell dynamics across first week of injury 19
2.5.3 NP administration enhances neuron sparing in spinal cord 20
2.5.4 NMJ sparing is enhanced by early NP administration 21
2.5.5 Early NP administration increases locomotor functional sparing 22
2.6 Discussion 23
Chapter 3 Nanoparticle and Epothilone D Combinatorial Intervention Improves Motor Performance and Regeneration in Chronic Cervical Spinal Cord Injury 27
3.1 Authors 27
3.2 Abstract 27
3.3 Introduction 28
3.4 Methods 30
3.5 Results 34
3.5.1 Nanoparticles improve motor function after chronic cervical injury 34
3.5.2 Epothilone D reduces scar tissue formation 35
3.5.3 Epothilone D improves axon regeneration 36
3.5.4 Epothilone D improves NMJ innervation in chronic injury 37
3.5.5 Nanoparticle and epothilone D combinatorial treatment enhances motor recovery 38
3.6 Discussion 39
Chapter 4 Conclusions and Future Directions 42
4.1 Summary of Findings 42
4.2 Significance and Impact 42
4.3 Future Directions 44
4.3.1 Investigation of Immune Cell Phenotype 44
4.3.2 Effects of NPs on astrocytes and endothelial cells 44

4.3.3 Nanoparticle design 45

4.3.4 Other models of SCI 45

Appendix 47

Bibliography 52

List of Figures

Figure 2.1: Immune cell infiltration in spinal cord at 7 dpi. Mice received daily injections of NPs or PBS control starting at varying times within first day of injury through intravenous injection for one week. Spinal cords were harvested at 7 dpi and IHC for macrophages (A) and neutrophils (B) was performed. Data are mean ± SEM. n=4-9 mice per condition. *p<0.05,**p < 0.01,***p<0.001 19

Figure 2.2 Immune cell population dynamics in spinal cord across first week of injury. Mice were given daily injections of NPs or PBS starting at 2 hours post-injury. Spinal cords were harvested at multiple timepoints across the first week of injury. Spinal cords were disassociated and myelin depleted before flow cytometry for immune cell surface markers for total immune cells (A), myeloid cells (B), macrophages and microglia (C), neutrophils (D), and monocytes (E). Data are mean ± SEM . n=5-6 mice per condition. *p < 0.05, **p < 0.01, *** p < 0.001, ****p < 0.0001 20

Figure 2.3 Neuron quantification contralateral to injury at 7 dpi. Mice received daily injections of NPs or PBS control starting at varying times within first day of injury through intravenous injection for one week. Spinal cords were harvested at 7 dpi and IHC was performed for neurons (A). Neurons contralateral to the C5 hemisection were quantified (B). Data are mean ± SEM. n = 5-7 mice per condition. *p < 0.05, *** p < 0.001, ****p < 0.0001.. 21

Figure 2.4 Neuromuscular junction innervation at 7 dpi. Mice received daily injections of NPs or PBS control starting at varying times within first day of injury through intravenous injection for one week. Muscles were harvested at 7 dpi and IHC was performed for axons (neurofilament medium chain, NFM) and motor endplates (bungarotoxin, BGT). (A). NMJs were quantified from the acromiotrapezius muscle (B-D) and flexor carpi ulnaris and flexor digitorum profundus (E-G). Data are mean ± SEM. n = 5-10 mice per condition. *p < 0.05, **p < 0.01, *** p < 0.001, ****p < 0.0001 22

Figure 2.5 Early NP treatment improves ladder beam performance. The horizontal ladder beam test was performed weekly following injury. The number of correct placements (A) and incorrect placements (B) were counted. Data are mean ± SD. n = 10 per condition. *p < 0.05 .. 23

Figure 3.1 Ladder beam performance in chronic injury model after NP administration. The horizontal ladder beam test was performed biweekly following injury. The number of correct placements (A,C) and incorrect placements (B,D) were counted out of 50 rungs after injury (A,B) and following bridge implantation (C,D). Data are mean ± SD. n = 8-12 mice per condition. * p < 0.05, **p < 0.01 35

Figure 3.2 Fibrotic and glial scarring at 4 weeks post-bridge implantation. Spinal cords were harvested 4 weeks post-bridge implantation. A) Representative image of glial and fibrotic scarring. B) EpoD reduces fibrotic scar tissue area. C) EpoD also reduces astrocytic scar formation. Data are mean ± SD. n=6 mice per condition. *p<0.05 **p<0.01 ***p<0.001 36

Figure 3.3 Axon growth and myelination into injury site at 12 weeks post-bridge implantation. Representative images of PBS+epo spinal cord (Ai) and NP+epo spinal cords (Aii). Total axons (B), axons myelinated by oligodendrocytes (C) and Schwann cells (D) were quantified by IHC. Data are mean ± SD. n=5-6 mice per condition. *p<0.05 37

Figure 3.4 Neuromuscular junction innervation at 12 weeks post-bridge implantation. The acromiotrapezius (A, C) and flexor digitorum profundus and flexor carpi ulnaris (B,D) were harvested 12 weeks after bridge implantation. Motor endplates (A,B) and innervated NMJs (C,D) were quantified by IHC. Data are mean ±SD. n=5-8 mice per condition. *p<0.05 **p<0.01 ***p<0.001 38

Figure 3.5 EpoD enhances motor function recovery in chronic injury after bridge implantation. The horizontal ladder beam test was performed biweekly following injury. The number of correct placements (A) and incorrect placements (B) were counted out of 50 rungs. Data are mean ±SD. n = 8-12 mice per condition. * p < 0.05 39

Figure A.1: Direct effects of NPs on immune cell trafficking. Flow cytometry for all adoptively transferred cells (A), adoptively transferred monocytes (b), and adoptively transferred neutrophils (c). Mean ± SD. *p<0.05, **** p<0.0001 51

Figure A.2: Indirect effects of NPs on immune cell trafficking. Flow cytometry for all adoptively transferred cells (a), adoptively transferred myeloid cells (b), adoptively transferred monocytes (c), and adoptively transferred neutrophils (d). Mean ± SD. *p<0.05 51

Abstract

Spinal cord injury (SCI) causes permanent loss of sensory and motor function below the level of injury due to neuronal death. Several extrinsic factors exacerbate the injury and limit the regenerative capability of the spinal cord. First, the infiltration of myeloid cells and the cytokines that they secrete exacerbate cell death and create a pervasive inflammatory environment. Second, fibroblasts and astrocytes migrate to the injury site and form scar tissue. Third, low expression of regeneration associated genes in the CNS and the presence of myelin debris and scar tissue inhibit axonal regeneration by neurons. To combat these issues, we proposed a combinatorial approach in both acute and chronic models of a cervical hemisection injury.

In an acute C5 hemisection model we investigated the window in time which poly(lactide-co-glycolide) nanoparticles (NPs) administration can successfully modulate the immune response and promote functional sparing. First, a microporous, multichannel poly(lactide-co-glycolide) PLG scaffold or "bridge" was implanted in place of the resected tissue. Second, NPs were injected intravenously following injury. These NP are phagocytosed by circulating monocytes and neutrophils, decreasing their migration to the SCI and reprogramming them towards an anti-inflammatory phenotype. At one-week post-injury, early NP intervention decreased the number of infiltrating macrophages and neutrophils but delaying treatment increased the number of neutrophils above control. All mice that received NPs had greater neuronal sparing contralateral to the injury, but mice that received NPs at early timepoints have greater neuromuscular junction innervation and motor endplate sparing. The increased sparing of

neurons and neural circuits in the early NP group corresponded with increased motor function, as measured by a ladder beam test. While mice in the late NP administration group initially performed poorly on the ladder beam test, their performance improved over time. Collectively, these results suggest that early intervention with NPs can modulate the inflammatory response and preserve motor function and circuits following SCI.

In a chronic C5 hemisection model, mice received PLG NPs for one week following injury to combat inflammation. Mice that received NP treatment made fewer mistakes on a ladder beam test of motor performance compared to control. At four weeks after injury, we resected scar tissue and inserted a microporous, multichannel PLG bridge. This removes inhibitory fibrotic and glial scar tissue and provides a scaffold to guide regenerating axons across the injury site. We then tested whether NP administration after the resection surgery can have a further beneficial effect. Mice that received NPs after both the initial injury and resection performed better on the ladder beam test than mice that received vehicle or NPs after only one surgery. Lastly, we administered epothilone D (epoD), a microtubule stabilizer that can penetrate the blood-brain barrier, to limit axon retraction and boost elongation. Mice that received epoD performed better on the ladder beam task than mice that did not, with mice that received both epoD and NPs performing best out of all experimental groups. Underlying this increased performance, all mice that received NPs or epoD exhibited robust axon growth into the injury and both oligodendrocyte and Schwann cell myelination of regenerating axons. Together, these results suggest that a combinatorial treatment plan that targets both inflammation and growth-inhibitory factors can improve motor performance following SCI.

Chapter 1 Overview of Spinal Cord Injury and Treatments

1.1 Significance

In the United States alone there are approximately 17,700 new cases per year and 288,000 people currently living with a spinal cord injury (SCI) [1]. SCI leads to permanent motor, sensory, bladder, and sexual dysfunction, thereby severely impacting the patient's quality of life and resulting in millions of dollars in lifetime healthcare costs per patient [2]. The average age of injury is 49 years, with peaks during adolescence and young adulthood and again later in life. Men are more likely to suffer a traumatic spinal cord injury with 79% of new injuries occurring in males since 2015. Cervical injuries are more common than thoracic (51% vs 36%) and more severely impact patient quality-of-life due to a greater degree of paralysis. Penetrating injuries only account for 14% of cases but cause greater functional deficits because the descending motor and ascending sensory tracts are severed [3]. The majority of new cases are contusion or compression injuries. Following SCI, spared axons that have some plasticity and sprouting ability can be found rostral to the injury. Sprouting can contribute to recovery following contusion or compression injuries, but in penetrating injuries axons never spontaneously cross a lesion to form functional connections caudal to injury [4-8]. Therefore, patients with penetrating SCI experience little, if any, improvement over time.

1.2 Pathology of Spinal Cord Injury

Spinal cord injury leads to permanent motor and sensory deficits due to the death of neurons and the limited regenerative ability of the central nervous system. In addition to the physical trauma of the initial injury, inflammatory myeloid cells infiltrate the spinal cord and

exacerbate neuron and oligodendrocyte death. Fibroblasts and activated astrocytes migrate to the injury site and secrete extracellular matrix proteins to form an astroglial scar. Scar tissue in addition to myelin debris from the injury inhibit axonal regeneration across the injury site. This series of events can be divided into an acute and chronic phase of SCI.

1.2.1 Acute Phase

The acute phase of SCI consists of the initial physical injury and the secondary injury. The acute and subacute phases of injury last from within minutes of injury until around 14 days post-injury in humans. The initial injury compresses or severs the spinal cord, directly damaging neurons and oligodendrocytes. The injury also damages the vasculature, which can compromise the blood-spinal cord barrier. The initial injury triggers an immediate inflammatory cascade that exacerbates damage.

1.2.2 Inflammatory response and secondary injury

Within 15 minutes of injury, resident microglia become activated and secrete pro-inflammatory cytokines like IL-1β and TNFα that attract circulating leukocytes to the injury[9]. Neutrophils, monocytes, and monocyte-derived macrophages are the primary immune cells that are recruited to the spinal cord injury. Neutrophil infiltration peaks at 1 day post-injury and persists for around 10 days[10]. Neutrophils help initiate inflammation through the release of pro-inflammatory cytokines, reactive oxygen and nitrogen species, and proteases. Monocyte infiltration is slower and peaks around one-week post-injury but can persist for over 6 months [11,12]. At the injury site, monocytes can differentiate into dendritic cells and macrophages, which both have pro-inflammatory and pro-regeneration phenotypes. During normal wound healing, macrophages initially take on a M1 or classically activated phenotype that is pro-inflammatory. M1-polarized macrophages are marked by secretion of inflammatory cytokines and chemokines

such as IL-1β, IL-6, IL-12, TNFα, and CCL2. As wound healing progresses, macrophages transition towards an M2 or alternatively-activated phenotype that is pro-regenerative. M2-polarized macrophages are marked by factors such as arginase-1, IL-10, IL-4, and TGF-β [13-15]. However, during SCI macrophages remain pro-inflammatory and the cytokines that they release exacerbate neuron excitotoxicity through upregulation of glutamate receptors [16,17]. Oligodendrocyte death causes demyelination of axons and deposition of myelin proteins, such as Nogo-A, myelin-associated glycoprotein (MAG), and oligodendrocyte myelin glycoprotein (OMgp), which are inhibitory to axon growth [18,19]. Therefore, the acute phase of injury exacerbates cell death and establishes a microenvironment that is inhibitory towards regeneration.

1.2.3 Subacute and Chronic Phases

The subacute and chronic phases of injury are marked by the formation and maturation of the glial scar. The subacute phase starts roughly two weeks following injury while the chronic phases starts several months later and persists indefinitely. In mice, fibroblasts start to migrate to the injury 5 days after injury and the fibrotic scar forms around the lesion core by 14 days after injury [20]. The release of ATP from damaged cells and inflammatory cytokines such as IFN-γ, TNFα, IL-1β, and IL-6 cause activation of astrocytes within hours of injury[21,22]. Astrocytes proliferate between one to 14 days after injury and form a tightly packed glial scar around the fibrotic core [23]. The astrocytes secrete a variety of ECM proteins with chondroitin sulfate proteoglycans (CSPGs) constituting the majority of the scar tissue. The glial scar functions to contain the injury, restore the blood-spinal cord barrier, and protect the surviving neural tissue from cytotoxic cytokines[24,25]. However, the CSPGs in the glial scar also act as a strong inhibitor of axon growth, causing growth cones to enter a dystrophic state or to deviate [26-29]. Due to the

inhibitory scar and lack of trophic support, axons fail to cross the injury and motor function is never recovered.

1.3 Clinical Interventions

Few clinical treatments exist for SCI. Following injury, surgical stabilization and decompression of the spinal cord may be required to reduce swelling and maintain cerebral blood flow [30]. Earlier decompression has been associated with increased clinical scores [31,32]. Methylprednisolone, a glucocorticoid, has been tested clinically to decrease inflammation after injury, but has yielded mixed results. Some patients saw increased clinical scores, but its use has been discontinued due to off-target side effects including sepsis, pneumonia, and impaired wound-healing [33-35]. Patients with incomplete SCIs may qualify for locomotor training on a treadmill, but the level and extent of the injury as well as the age of the patient play a major role in the effectiveness of this therapy. While younger patients with lower SCIs have seen benefit to locomotor training, older patients and those with higher SCIs see little improvement [36,37]. Electrical stimulation is a promising treatment that can be paired with motor training. The stimulation can be percutaneous, transcutaneous, epidural, or intraspinal and aims to stimulate surviving circuitry and promote neuroplasticity. With electrical stimulation patients have been able to stand and walk unassisted [38-41]. However, this technology is experimental with relatively few participants.

1.4 Experimental Therapies

Many experimental strategies have been developed to promote regeneration following spinal cord injury. The main categories of treatments are pharmacological agents, gene therapy, cell transplantation, and biomaterials. Pharmacological agents can address various causes of and symptoms of spinal cord damage. Methylprednisolone and tirilazad have been used to decrease

the inflammatory response to injury[42]. The GABA receptor agonists baclofen and pregabalin can be used to reduce muscle spasticity and neuropathic pain following SCI[43,44]. Although these drugs may provide some beneficial effects to patients, they often have side effects that are not well-tolerated. Gene therapy, often through viral vectors such as lentivirus, adenovirus, and adeno-associated virus, can be used to express neurotrophic and growth factors within the spinal cord[45,46]. While neurotrophic factors can promote regeneration, they can deteriorate, and repeated intrathecal injections carries risk of further injury. Therefore, expression of these growth factors through viral-mediated gene therapy is a promising approach. Cell transplantation can be used to replace oligodendrocytes, neurons, and astrocytes that have died after SCI. Neural stem cells that have the ability to differentiate into these cell types are commonly investigated. Studies have reported greater motor recovery following stem cell transplantation, but stem cells can be prone to both immune rejection or uncontrolled proliferation[47-49]. This dissertation focuses on the use of biomaterials in both nanoparticles and scaffolds that bridge the injury and the microtubule-stabilizing agent epothilone D.

1.4.1 Biomaterials

Biomaterials are used to provide structure and support to the injury to prevent scar and cyst formation and promote regeneration. A variety of biomaterials have been investigated including naturally-occurring materials, such as laminin, collagen, hyaluronic acid, alginate, and chitosan, and synthetic materials like polylactic acid (PLA), polyethylene glycol (PEG), and poly(lactide-co-glycolide) (PLG) [50-56]. While naturally occurring biomaterials may be more biocompatible and biodegradable, synthetic biomaterials have more tunable properties. Synthetic materials can be engineered to have desired biodegradability, stiffness, porosity, and

architecture. Additionally, polymers can be more easily modified for localized delivery of proteins or growth factors [57,58].

The Shea lab has previously developed a PLG bridge that is designed to be inserted into a hemisection SCI model [59]. PLG has been approved by the FDA for human use for decades for sutures, drug delivery, and as a matrix for cell transplantation and degrades into lactic acid and glycolic acid via hydrolysis. The bridge is made using PLG microspheres mixed with salt in a mold along with sugar strands. The salt provides microporosity to the bridge that allows for cellular infiltration. We have previously found oligodendrocytes, Schwann cells, and macrophages in the bridge [60,61]. The sugar strands act as a template for channels that act as conduits for both motor and sensory nerve growth. The slow degradation time of the bridge allows for cellular infiltration and integration with the spinal cord tissue during healing but also delineates a distinct injury area that is useful for studying regenerating axons. We have also used the bridge as a method to deliver stem cell progenitors and lentivirus encoding anti-inflammatory cytokines and neurotrophic factors[46,62-64].

1.4.2 Nanoparticles

Like biomaterials, nanoparticles (NPs) are a highly customizable platform for SCI treatment. While drugs like methylprednisolone and paclitaxel show promise in the treatment of SCI, their bioavailability in the spinal cord is limited due to their inability to cross the blood-spinal cord barrier [65,66]. Growth factors, peptides, and neurotrophic factors have also been widely investigated for use in SCI, but their rapid clearance limits their efficacy. NPs provide a platform for delivering these drugs or growth factors across the blood-spinal cord barrier and increase the concentration of the therapeutic agent at the injury site [67,68]. NPs can be made from a variety of materials including inorganic metals like gold, manganese oxide, or cerium oxide [69-71], naturally

occurring biomaterials like chitosan [72], or polymers like PLG or PEG[73-75]. While therapeutic agents can be conjugated to NPs, some formulations of NPs have therapeutic benefit themselves. The Shea lab has previously shown that cargo-less PLG NPs have the ability to redirect immune cell trafficking away from a thoracic SCI, alter the phenotype of neutrophils and macrophages to be less inflammatory, and improve motor function recovery [76].

1.4.3 Epothilones and Microtubule Stabilizers

Microtubule organization plays an important role in both scar tissue formation and axon retraction following SCI. Following transection, axons in the peripheral nervous system can form growth cones with organized microtubules that are capable of sustained elongation. In contrast, transected axons in the central nervous system form retraction bulbs on the proximal stump that enlarge over time due to disorganized and depolymerized microtubules[77,78]. When treated with the microtubule-destabilizing drug nocodazole, severed dorsal root ganglia neurons form retraction bulbs similar to those seen in the central nervous system, proving that microtubule stabilization is important for axonal regeneration[79].

Paclitaxel, a popular microtubule stabilizing chemotherapeutic agent, has been previously shown to limit scar tissue formation and promote axon elongation, however it cannot cross the blood-spinal cord barrier [80,81]. To circumvent this, paclitaxel has been conjugated to hydrogels or NPs to allow it to reach the injured spinal cord, but these methods have not yet been approved clinically [82-85]. Epothilones are a class of FDA-approved microtubule-stabilizing agents that have been previously approved for use in triple-negative breast cancer [86,87]. Unlike paclitaxel, epothilones have the ability to cross the blood-spinal cord barrier and have been investigated for use in diseases such as Alzheimer's disease, Amyotrophic Lateral Sclerosis, and TBI [87-89]. Epothilones B and D have been shown to decrease fibrotic scar formation and increase axon

elongation following SCI. Axon elongation is thought to occur through microtubule stabilization that limits the formation of retraction bulbs. Fibrotic scar tissue is not reduced due to fibroblast cell death or lack of growth. Instead, microtubule stabilization prevents meningeal fibroblast migration to the injury site by removing cell polarization[90]. The ability of epothilones B and D ability to enhance motor function, however, has shown mixed results and remains unclear [90-93].

1.5 Models of Spinal Cord Injury

A variety of animal models exist for SCI research, including rat, mouse, cat, pig, and nonhuman primate models. Nonhuman primates are sometimes used in research due to their similarity to humans with respect to size of axons, spinal cord tract anatomy, and inflammatory response to injury [94-97]. However, these nonhuman primate studies are not prevalent due to ethical and budgetary concerns. Instead, the majority of studies use rat or mouse models due to their availability and cost-effectiveness compared to larger animal models. Rats more closely mimic human spinal cord injuries in regard to cystic cavity formation during the chronic phase of SCI [10,98]. In contrast, mice form a dense inflammatory and fibrotic core at the center of the SCI. The timeline of macrophage infiltration to the injury is similar between rats and mice, but neutrophil infiltration can persist for 7-14 days in mice compared to 3 days in rat[99,100]. Mice are more commonly used because of the wide availability of transgenic strains that can help elucidate mechanisms underlying SCI pathology[101].

SCI models can also be categorized by the type of injury. The main types of injury are transection, contusion, and compression. Transection models have high replicability and allow the investigation of biomaterial scaffolds that bridge the injury[102]. Contusion models involve a transient physical impact to the spinal cord whereas compression models involve an applied force to the spinal cord for a brief duration of up to several minutes. Contusion injuries are

commonly caused by weight drops or electromagnetic impactors where the weight or force applied to the spinal cord is proportional to the severity of the injury[10,102]. In compression injuries, the severity of injury can be modulated by using aneurysm clips with varying closing forces[103,104].

In this dissertation, we used a mouse cervical hemisection model. A mouse model was used because of the availability of transgenic mouse strains and a cervical model used because the majority of human SCI cases occur at the cervical level[1]. A hemisection model was chosen to allow for the investigation of axonal regeneration through our PLG bridge. While contusion injuries are more common, patients that have penetrating or transection injuries exhibit little spontaneous recovery following injury and there are no current clinical treatments that are designed to reconnect the severed spinal cord[105,106].

1.6 Thesis Overview

Spinal cord injury results in permanent motor and sensory deficits, including paralysis and loss of bladder, bowel, and sexual function. Due to the limited regenerative capacity of the central nervous system and extrinsic factors such as inflammation and scar tissue formation, repairing a SCI is a difficult clinical challenge. The studies presented here investigate treatments to reduce inflammation and promote regeneration following injury using a combination of polymer nanoparticles, biomaterial bridges, and microtubule stabilizing agents to attain functional recovery.

Chapter 1 describes the pathology and phases of spinal cord injury. Current clinical treatment and experimental therapies including nanoparticles (NPs), biomaterials, and microtubule stabilizers are also discussed.

Chapter 2 investigates the role of timing of nanoparticle administration during the first week of injury on functional recovery following a cervical hemisection. NPs when delivered within 24 hours of injury, retain the ability to modulate the inflammatory microenvironment and promote greater functional recovery. Early administration best attenuates inflammation and functional deficits, but later administration is associated with improvement of function over time.

Chapter 3 investigates the use of nanoparticle therapy in a chronic cervical hemisection model. NPs alone are able to promote functional recovery following chronic SCI. When combined with epothilone D (epoD), a microtubule stabilizer, NPs are able to limit glial and fibrotic scar formation, promote axon growth and myelination in the injury site, promote neuromuscular junction innervation, and further improve motor recovery. Together, these results support the need for a combinatorial approach to SCI treatment that can reduce acute inflammation while promoting chronic regeneration.

Chapter 4 summarizes the results, discusses future research directions, and concludes the dissertation.

Appendix A describes an adoptive transfer study of myeloid cells to investigate the direct and indirect effects of PLG nanoparticles on immune cell trafficking to the injured spinal cord. When incubated directly with NPs, NP-positive immune cells decrease their infiltration to the spinal cord compared to NP-negative immune cells. When administered to injured mice, NPs can influence the SCI microenvironment to indirectly decrease accumulation of transferred immune cells.

Chapter 2 Early Nanoparticle Intervention Preserves Motor Function Following Cervical Spinal Cord Injury

2.1 Authors

Sarah E. Hocevar, Brian C. Ross, Yinghao Wang, Cecelia R. Crowther, Samantha R. Schwartz, Brain J. Cummings, Aileen J. Anderson, Lonnie D. Shea

2.2 Abstract

Spinal cord injury (SCI) triggers an immediate influx of immune cells that secrete pro-inflammatory cytokines and reactive oxygen species that cause tissue damage that is secondary to the initial physical trauma. We aim to reprogram these immune cells to promote a less inflammatory and more pro-regenerative environment. Herein, we investigated the window in time which poly(lactide-co-glycolide) (PLG) nanoparticles (NPs) administration can successfully modulate the immune response and promote functional sparing. The dynamics of immune cell infiltration and secondary tissue damage were studied following injection of NPs intravenously every 24 hours for 7 days following injury with the first injection starting at 2-, 4-, or 24-hours post-injury (hpi). At 7 days post-injury (dpi), early NP intervention decreased the number of infiltrating macrophages and neutrophils but delaying treatment until 24 hpi increased the number of neutrophils above control. All mice that received NPs had greater neuronal sparing contralateral to the injury, but mice that received NPs at early timepoints have greater neuromuscular junction innervation and motor endplate sparing. The increased sparing of neurons and neural circuits in the 2 hpi NP group corresponded with increased motor function, as

measured by a ladder beam test. Collectively, these results suggest that early intervention with NPs can modulate the inflammatory response and preserve motor function and circuits following SCI.

2.3 Introduction

The United States alone has approximately 17,000 new cases of spinal cord injury (SCI) each year [1]. Following injury, circulating neutrophils infiltrate the spinal cord within hours of injury and release inflammatory cytokines and reactive oxygen and nitrogen species at the injury that exacerbate neuronal and oligodendrocyte cell death [107-109]. Methylprednisolone, a glucocorticoid that downregulates adhesion molecule and cytokine production in immune cells, has been investigated in clinical trials to decrease the inflammatory response to SCI [33-35]. However, while some patients exhibited improved motor and sensation function, its use has been discontinued because of its many off-target effects including sepsis, pneumonia, impaired wound healing, and gastrointestinal bleeding. Additionally, mouse studies have shown that complete ablation of neutrophils and macrophages does not significantly improve motor performance and has a negative effect on wound healing and regrowth into the injury [110-112]. Together, these studies demonstrate the need for a clinical intervention that can attenuate immune cells during spinal cord injury without causing widespread immunosuppression and its negative effects.

An emerging strategy for SCI to address inflammation is polarizing innate immune cells toward a less-inflammatory phenotype, which can lead to phenotypes that promote rather than diminish functional recovery. Biomaterial technologies in particular have emerged as tools to locally modulate inflammation and enhance the regenerative potential of the spinal cord. Recently nanoparticles (NPs) have been reported to target spinal cord injury due to their ability to cross the semipermeable blood-brain barrier [67,68]. Nanoparticles are often conjugated to a therapeutic agent

and administered systemically, yet limited accumulation of NPs at the injury limits the extent of the therapeutic effect. Conjugating additional guiding peptides onto the NPs can increase accumulation in the spinal cord, but the therapeutic effect can still be limited by the low phagocytic ability of many resident cells of the spinal cord [113-116]. To circumvent these accumulation issues and the off-target effects of drugs like methylprednisolone, our lab has previously developed cargo-less poly(lactide-co-glycolide) (PLG) NPs that are phagocytosed by circulating myeloid cells and reprograms them toward a more anti-inflammatory phenotype. Administration of these NPs led to an improved functional recovery in mice as early as 7 days post injury that were sustained for at least 12 weeks [76].

In this report, we investigate the cellular processes that are influenced by NP administration, with assessment of the immune dynamics following administration, and sparing of neural tissue. The studies employ a cervical injury, and the timing of initial NP administration was varied between 2 and 24 hours after injury, with daily NP injections subsequently for one week. The varied timing of first NP administration was anticipated to target different populations of infiltrating immune cells. An administration time of 2 hours would target neutrophil and monocyte populations that are upregulated following injury, whereas a 4-hour time point would preferentially target monocytes [117,118]. An administration time of 24 hours was chosen because both neutrophils and monocytes have already begun to accumulate in the injury [13]. While the numbers of infiltrating immune cells are similar in NP-treated and control mice 2 days post-injury, fewer cells were present by the end of the first week post-injury in mice that received early NP treatment. All NP conditions led to increased survival of neurons in the spinal cord compared to controls, but earlier intervention improved neuromuscular junction innervation (NMJ) and motor performance.

Collectively, these results support the use of NPs as a means to modulate the acute inflammatory response to improve outcomes in spinal cord injury.

2.4 Methods

PLG NP fabrication and administration

PLG NPs were made by dissolving 50:50 PLG (inherent viscosity = 0.55dL/g; Evonik, Sand Creek, MI) in dichloromethane along with poly(ethylene-alt-maleic anhydride) (PEMA) (Polysciences, Inc., Warrington, PA). The mixture was sonicated with a Cole-Parmer CPX130 Ultrasonic Processor (Vernon Hills, IL) and then stirred overnight to evaporate the organic phase. The following day the NPs were collected and washed with water to produce particles that are approximately 500 nm in diameter and have a zeta potential from -40 to -60 mV. Particle size and charge were measured with a Zetasizer Nano ZSP (Malvern Panalytical, Malvern, United Kingdom). The particles were lyophilized with sucrose and D-mannitol (Sigma-Aldrich, St. Louis, MO). During administration, each mouse received 0.1 mL of 10 mg/mL NPs in DPBS injected into the lateral tail vein daily for one week following injury. Control mice received 0.1 mL DPBS instead of NPs. The timing of the first NP injection varied from 2 hours post-injury (hpi) up to 24 hpi.

Multichannel PLG bridge fabrication

Bridges were fabricated using the same protocol previously published by our lab [45,46,60]. PLG (75:25 lactide:glycolide; inherent viscosity = 0.76 dL/g; Lakeshore Biomaterials, Birmingham, AL, USA) was dissolved in dichloromethane (6 % w/w) and emulsified in 1% poly (vinyl-alcohol) (Millipore Sigma, Burlington, MA) using a homogenizer (PolyTron 3100; Kinematica AG, Littau, Switzerland). The resulting microspheres were approximately 1 um in diameter. D-sucrose (Millipore Sigma), D-glucose (Millipore Sigma), and dextran MW 100,000 (Millipore

Sigma) were mixed at a ratio of 5.3:2.5:1, respectively, by mass and then were caramelized, cooled, and drawn from solution using a Pasteur pipette to create sugar strands. Each 150-250 um strand was coated with a 1:1 mixture of PLG microspheres and salt (63–106 mm) and pressed into a salt-lined aluminum mold. The strands were used to create channels to act as a conduit for regenerating axon bundles and salt was used to create a microporous structure. The materials were gas-foamed under 800 psi for 16 hours to fuse the particles into a matrix. The bridges were cut into 1.15 mm long pieces and the NaCl was leached with water, leaving behind a multichannel bridge.

Spinal cord hemisection model and animal care

All animal work was performed according to protocol number PRO00011456 approved by the Institutional Animal Care and Use Committee (IACUC) at the University of Michigan. A C5 lateral hemisection was performed on 6-8 week old male and female C57BL/6J (Jackson Laboratory, Bar Harbor, ME) or Crym-RFP (cross between Mutant Mouse Resource & Research Center #036627-UCD and Jackson Laboratory #007905) mice as previously described [45]. Briefly, mice were anesthetized with 2% isoflurane and 1 mg/kg bupivacaine was administered as a local anesthetic. After a C5 laminectomy was performed, a 1.15 mm lateral hemisection of the left side of the spinal cord was removed to allow for PLG bridge implantation. The injury and exposed spinal cord were covered in Gelfoam (Ethicon, Raritan, NJ). Muscles were sutured using 5/0 Chromic Gut (Henry Schein, Melville, NY), and the skin was stapled. Post-operative care consisted of buprenorphine (0.1 mg/kg) twice daily for 3 days, enrofloxacin (2.5 mg/kg, Bayer, Leverkusen, Germany) daily for 14 days, and lactated ringers' solution (1 mL, MWI Veterinary Supply, Boise, ID) daily for 5 days. Bladders were expressed twice daily until function recovered and wound clips were removed 10 days after surgery.

Behavioral analysis

The horizontal ladder beam test was used to evaluate locomotor function over a period of 12 weeks following injury. Mice were trained on the ladder beam consisting of 50 rungs during the week prior to injury. Mice were recorded at 1, 2, and every two weeks up to 12 weeks following injury. Videos were scored by two blinded observers for 3 trials per animal by counting the number of correct and misplaced steps of the left forepaw on the ladder beam.

Immunohistochemistry

At 1-week post-injury, mice were euthanized with 5% isoflurane and C4-C6 along with the left acromiotrapezius and forearm flexor muscles were dissected. Tissues were flash frozen in isopentane on dry ice and embedded in 20% w/w sucrose (Millipore Sigma) in OCT (Thermofisher Scientific). Muscles and spinal cords were cryosectioned at 14 um thick longitudinally and transversely, respectively. Tissue sections were permeabilized in 0.5% Triton in Tris-buffered saline, fixed with 4% paraformaldehyde, and blocked with normal goat or normal donkey serum as necessary.

Antibodies used were mouse anti-NeuN (1:250, Millipore, Burlington, MA, #MAB377) for mature neurons, chicken anti-NF200 (1:250, AVES Labs, Davis, CA, #NFH) for neurofilaments, anti-bungarotoxin conjugated to Alexa Fluor 647 (1:500, Thermo Fisher, Waltham, MA, #B35450) for motor endplates, rat anti-F4/80 (1:200, Bio-rad MCA497GA) for macrophages, and rat anti-Ly6G (Biolegend #127602) for neutrophils.Secondary antibodies were AlexaFluor 555 goat anti-rat (1:1000; Invitrogen #A21434), AlexaFluor 555 goat anti-mouse (1:1000; Invitrogen #A21424), and AlexaFluor 488 goat anti-chicken (1:1000; Invitrogen #A11039). Tissues were imaged on an Axio Observer Z1 using an ORCA-Flash 4.0 V2 Digital CMOS camera.

Quantification of IHC

To quantify immune cells in the spinal cord, images were exported as .CZI files and converted to .H5 files in CellProfiler [119]. The injury area was outlined using the polygon tool in Fiji and saved as a mask [120]. The .H5 files were uploaded to Ilastik and pixel classification was performed after training a set of 4 randomly selected tissues per condition [121]. A single operator trained Ilastik to ensure consistent staining identification and the program was trained against a no primary control to prevent identification of non-specific staining. Immune cells were identified by colocalization of greater than 3 pixels of either F4/80 for macrophages/microglia or Ly6G for neutrophils with DAPI. Only immune cells in the injury area were counted.

The number of NeuN+ neurons on the C5 uninjured side of the spinal cord contralateral to the injury were manually counted by two independent, blinded observers using Fiji. Density of innervated NMJs, density of motor endplates, and fraction of innervated NMJs were manually calculated by two independent, blinded observers using Fiji.

Flow cytometry

At 2, 5, or 7 dpi, mice were euthanized with 5% isoflurane and C4-C6 of the spinal cord was dissected, including both the injury site and contralateral side. For uninjured controls, C4-C6 was also dissected. Trypsin (0.5 mg; Millipore Sigma) and collagenase (1 mg; Millipore Sigma) in DMEM were added to a tube with the spinal cords and the spinal cords were minced with microscissors. Following mincing, tissues were incubated at 37 C in a rotisserie shaker for 20 minutes. The samples were spun down at 500g in a microcentrifuge and neutralized with DMEM with 10% FBS (Thermofisher Scientific). The samples were spun down again and supernatant aspirated. Then the tissues were myelin depleted using the Miltenyi Myelin Removal Beads II kit (Bergisch Gladbach, Germany). Following myelin depletion, cells were counted and 1 million

cells per animal were used for flow cytometry. Fixable Live/Dead Violet was used to assess cell viability. Samples were incubated with anti-CD16/32 (1:100, clone 93; Biolegend) to block nonspecific staining. Cells were additionally incubated with antibodies for CD11b BV421 (0.2 ug/uL; Biolegend 101251) Ly6C BV510 (0.1 ug/uL; Biolegend 128033), Ly6G PE (0.2 ug/uL; Biolegend 127608), F4/80 AF647 (0.5 ug/uL; Biolegend 157314), and CD45 FITC (0.5 ug/uL; Biolegend 103108) and analyzed using a BioRad ZE5 Cell Analyzer. Data analysis was performed using FlowJo (BD).

Statistical Analysis

Statistical analysis was performed in Graphpad Prism 10. All values are expressed as the mean ± standard error of the mean. For flow cytometry n=5-6 mice were used. For immunohistological data, n=4-10 mice were used. Number of mice used in a specific figure is noted in the figure caption. For flow cytometry and immunohistochemistry, an ordinary one-way ANOVA was used with Tukey's post-hoc test to correct for multiple comparisons. For ladder beam data, n=10 mice were used and a two-way ANOVA with Tukey's post-hoc test was performed. The p-values for statistical significance are represented with stars (Unless otherwise noted: *$p < 0.05$, **$p < 0.005$, ***$p < 0.0005$, ****$p < 0.0001$).

2.5 Results

2.5.1 Nanoparticle administration alters immune infiltration into the spinal cord

The initial studies analyzed the composition of immune cell populations in the spinal cord at one-week post-injury. We investigated the efficacy of NPs when the initial administration occurs at distinct time points following injury, which may reflect the delays in treatment that may be present in a clinical situation. NP were initially administered at 2-, 4-, and 24-hours post-injury (hpi), with daily administration subsequently until one week. At 7 days post-injury (dpi), spinal cords were

harvested, and immune cell infiltration was quantified by immunohistochemistry for F4/80+ macrophages/microglia (Figure 2.1A) and Ly6G+ neutrophils (Figure 2.1B). Consistent with our previous studies, NP administration starting within 2 hpi trended toward a decrease in the number of F4/80+ macrophages/microglia and Ly6G+ neutrophils compared to PBS controls. Interestingly, delayed NP injections starting at 24 hpi resulted in higher Ly6G+ neutrophil ($p=0.0046$) infiltration than the PBS control.

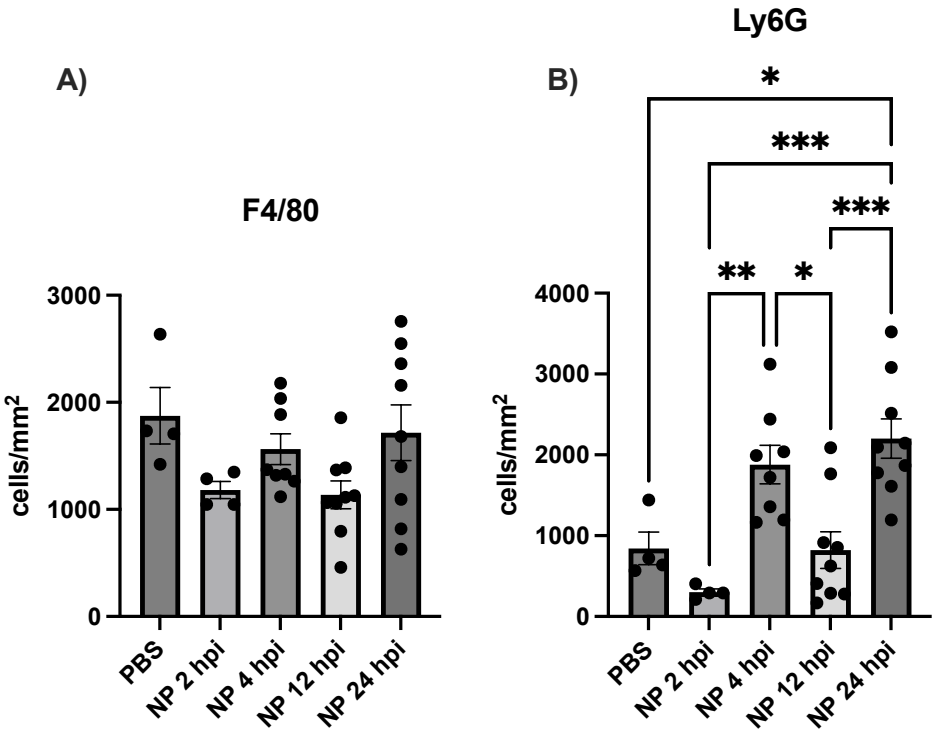


Figure 2.1: Immune cell infiltration in spinal cord at 7 dpi. Mice received daily injections of NPs or PBS control starting at varying times within first day of injury through intravenous injection for one week. Spinal cords were harvested at 7 dpi and IHC for macrophages (A) and neutrophils (B) was performed. Data are mean ± SEM. n=4-9 mice per condition. *p<0.05,**p < 0.01,***p<0.001

2.5.2 Immune cell dynamics across first week of injury

Next, we further analyzed the immune cell response in the spinal cord throughout the first week of injury with and without NP intervention. Mice received NPs or PBS starting within 2 hpi and flow cytometry was performed at 2, 5, or 7 dpi. NP administration trended toward a lower

percentage of total CD45+ cells in the spinal cord compared to the PBS control at 5 dpi (p= 0.0701) (Figure 2.2A). The percentage of CD11b+ myeloid cells significantly increased across the first week for PBS-treated mice (p=0.0116), yet not for NP-treated mice (p=0.6860) (Figure 2.2B). At 5 dpi, the percentage of myeloid cells was significantly lower in mice that received NPs (p=0.0222). Within each condition, the percentage of F4/80+ cells (macrophages and microglia) increased across the week, and by day 7, significantly fewer F4/80+ cells were observed in mice that received NPs (p= 0.0207) (Figure 2.2C). The percentages of Ly6G+ neutrophils (Figure 2.2D) and Ly6C+ monocytes (Figure 2.2E) decrease across the first week within each condition and at day 5 are lower in NP-treated mice. In total, these results show that NPs are able to decrease the accumulation of innate immune cells across the first week after injury.

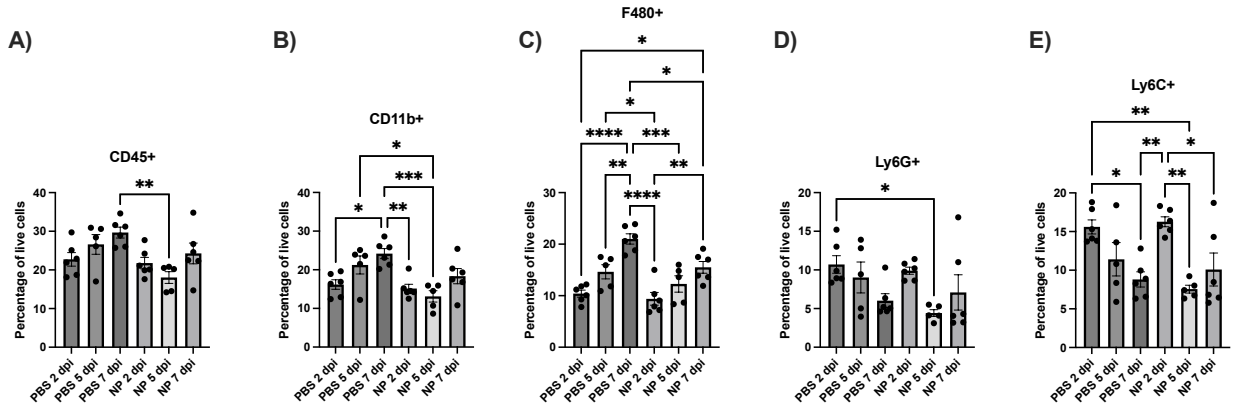


Figure 2.2 Immune cell population dynamics in spinal cord across first week of injury. Mice were given daily injections of NPs or PBS starting at 2 hours post-injury. Spinal cords were harvested at multiple timepoints across the first week of injury. Spinal cords were disassociated and myelin depleted before flow cytometry for immune cell surface markers for total immune cells (A), myeloid cells (B), macrophages and microglia (C), neutrophils (D), and monocytes (E). Data are mean ± SEM . n=5-6 mice per condition. *p < 0.05, **p < 0.01, *** p < 0.001, ****p < 0.0001

2.5.3 NP administration enhances neuron sparing in spinal cord

We next hypothesized that NP delivery has the ability to influence neuron sparing within the injured spinal cord. Following spinal cord injury, inflammation and excitotoxicity resulting from the trauma and inflammatory cytokine release can induce widespread neuron death.

Immunohistochemistry was performed at 1 wpi for NeuN+ mature neurons within the contralateral side to the injury, where inflammatory cytokine concentration should be highest (Figure 2.3A, circled in yellow). All injured conditions had fewer neurons than uninjured controls, and NP administration starting at 2- and 4- hours post-injury trended toward increased neuron count compared to the PBS control ($p = 0.0521$ and 0.0145) (Figure 2.3B).

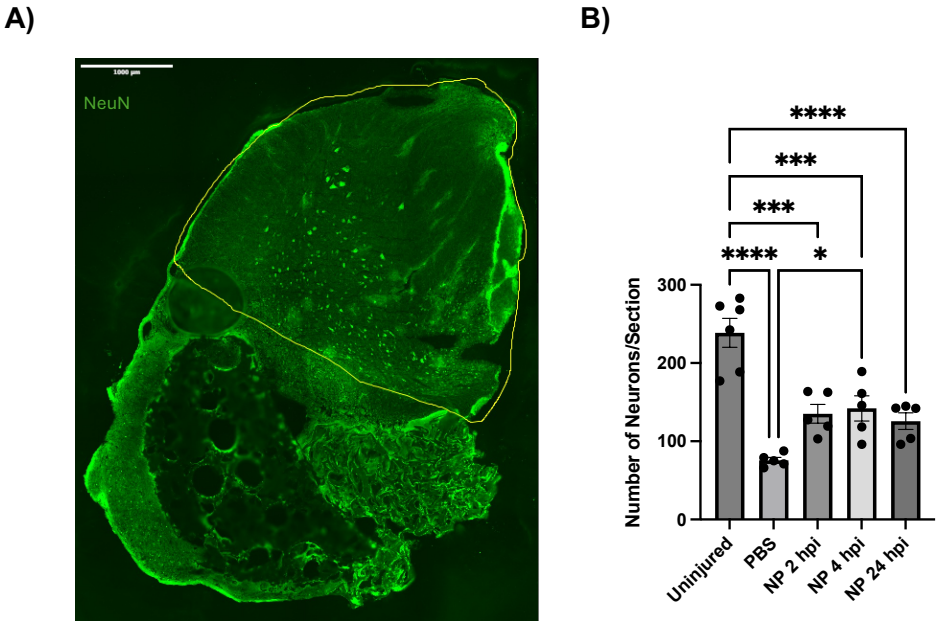


Figure 2.3 Neuron quantification contralateral to injury at 7 dpi. Mice received daily injections of NPs or PBS control starting at varying times within first day of injury through intravenous injection for one week. Spinal cords were harvested at 7 dpi and IHC was performed for neurons (A). Neurons contralateral to the C5 hemisection were quantified (B). Data are mean ± SEM. n = 5-7 mice per condition. *$p < 0.05$, *** $p < 0.001$, ****$p < 0.0001$

2.5.4 NMJ sparing is enhanced by early NP administration

We next investigated the correlation between NP administration and the sparing of neural circuits. These circuits were quantified in the muscle of the acromiotrapezius (ATX) and forearm flexor muscles through IHC for bungarotoxin+ (BGT+) motor endplates and neurofilament 200+ axons (NFM+) (Figure 2.4A). SCI can cause the death of lower motor neurons, causing the denervation of NMJs. Prolonged loss of synaptic input leads to the disintegration of orphaned motor endplates and muscle atrophy [122-125]. The ATZ is innervated from C5 and therefore directly affected by the

injury (Figure 2.4B-D), whereas the flexor muscles are innervated from C6 below the injury (Figure 2.4E-G) [126]. In the ATZ, NP treatment did not significantly increase sparing of NMJs. However, in the flexor muscles, early NP treatment starting at 2 hpi had a significantly greater percentage of innervated motor endplates compared to control (p=0.0004). NP treatment may not be able to spare NMJ innervation that is associated with the hemisection, but it can help spare innervation caudal to the injury site.

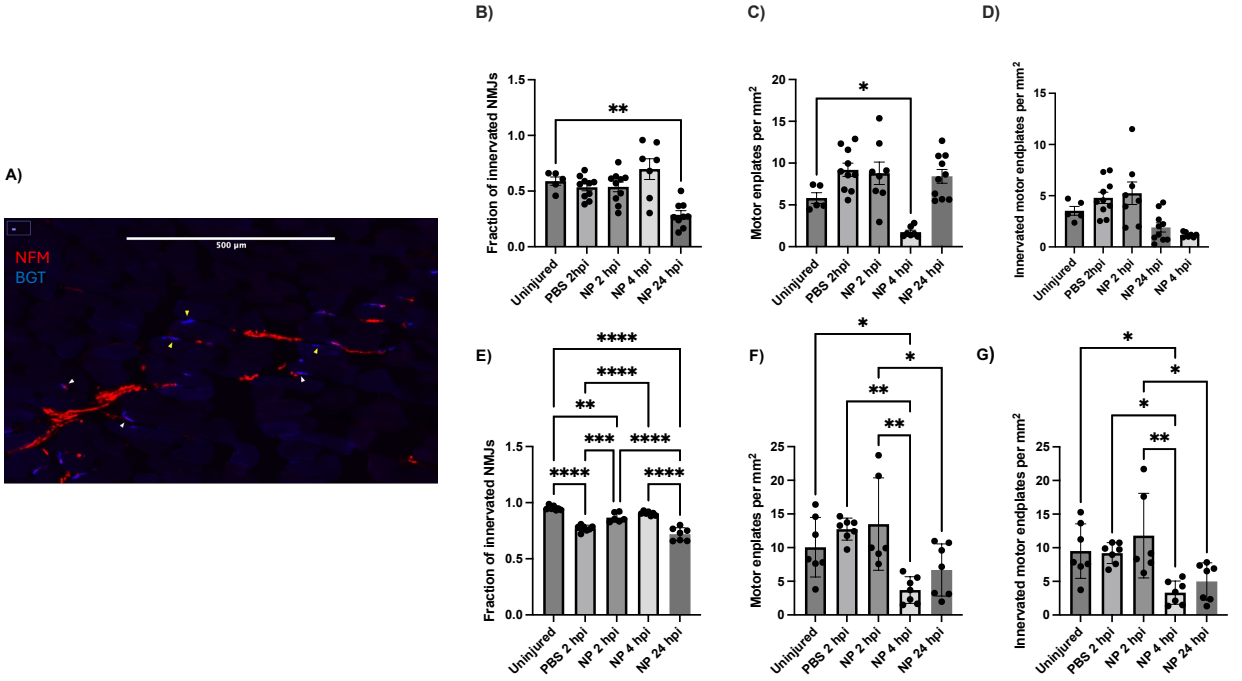


Figure 2.4 Neuromuscular junction innervation at 7 dpi. Mice received daily injections of NPs or PBS control starting at varying times within first day of injury through intravenous injection for one week. Muscles were harvested at 7 dpi and IHC was performed for axons (neurofilament medium chain, NFM) and motor endplates (bungarotoxin, BGT). (A). NMJs were quantified from the acromiotrapezius muscle (B-D) and flexor carpi ulnaris and flexor digitorum profundus (E-G). Data are mean ± SEM. n = 5-10 mice per condition. *p < 0.05, **p < 0.01, *** p < 0.001, ****p < 0.0001

2.5.5 Early NP administration increases locomotor functional sparing

Mice underwent a horizontal ladder beam test to investigate whether the spared neurons and NMJs in the NP conditions correlated with better locomotor function. At 7 dpi, mice that received NPs within 2 hpi performed significantly better than PBS controls and other NP conditions with more correct placements (NP 2 hpi vs PBS: p = 0.0342) (Figure 5A) and fewer missed rungs (NP 2 hpi

vs NP 4 hpi, NP 24 hpi: p = 0.0037, 0.0112) (Figure 5B). Mice that did not receive NPs until 24 hpi performed similarly to mice that only received PBS. Mice that received NPs at the intermediate timepoint of 4 hpi performed worse than the 2 hpi group, but better than the PBS and NP 24 hpi group. After 7 dpi, the motor performance of the NP 2 hpi condition remained steady, but the other NP conditions improved over 6 weeks. The performance of the PBS group did not significantly change over the course of the experiment. Collectively, NP administration improved locomotor recovery during the acute and subacute phases of injury if administered within 4 hours after SCI.

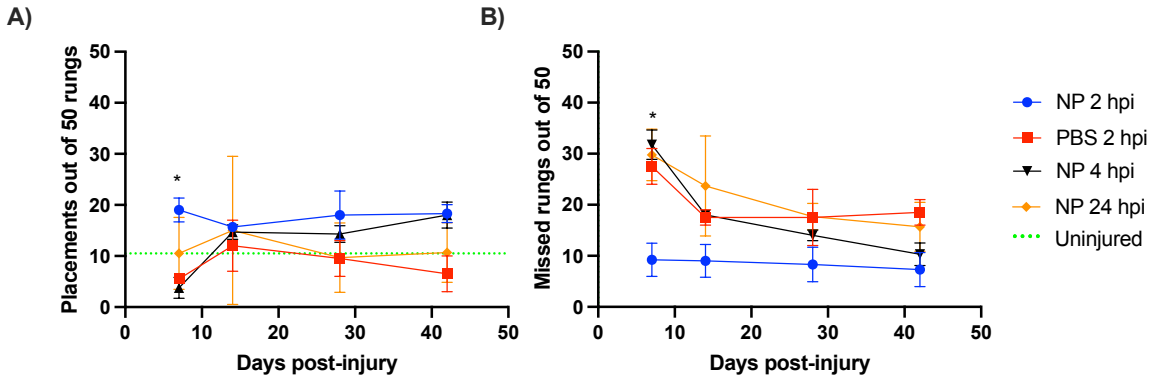


Figure 2.5 Early NP treatment improves ladder beam performance. The horizontal ladder beam test was performed weekly following injury. The number of correct placements (A) and incorrect placements (B) were counted. Data are mean ± SD. n = 10 per condition. *p < 0.05

2.6 Discussion

In these studies, we investigated the use of NPs to reprogram circulating immune cells to enhance regeneration and functional recovery after spinal cord injury. Spinal cord injury leads to the activation of innate immune cells, such as inflammatory monocytes and neutrophils, in the blood and spleen, which can subsequently traffic to the injured spinal cord [127,128].This infiltration into the SCI can induce damage secondary to the initial injury, thereby contributing to neuronal cell death, axonal dieback, demyelination, and scar tissue formation [117,129]. Studies that have attempted depletion of these circulating cells have indicated worsened histological and functional outcomes [110]. NPs, in contrast, do not function to deplete immune cells and instead reprogram their

function. After injury, the activated innate immune cells, which have high phagocytic capacity for scavenging cell debris and foreign materials, can internalize the NPs while in circulation. This internalization of the NPs can alter the trafficking and functional phenotype of the innate cells [130], which has led to improved functional recovery [76]. The immune response following SCI can be highly dynamic, and herein we investigated the timing of NP administration.

NP administration, regardless of the timing for the initial administration, had a different immune cell composition in the spinal cord at 1 week post injury. Previous reports had indicated that NPs delivered at 2 hours post injury decreased the number of inflammatory monocytes and neutrophils at 1 week post injury [76]. Herein, we observed a decreased number of macrophages within the injury for all mice that received nanoparticles. Interestingly, mice that received NPs within 4 hours of injury also had fewer neutrophils in the spinal cord, yet mice receiving particles starting at 24 hpi had greater accumulation of neutrophils at 1 week relative to control. Analyzing responses over time, only NP administration at 2 hpi resulted in a smaller percentage of myeloid cells at 2, 5, and 7 dpi. The immune cell dynamics play an important role in the response that leads to their repair or regeneration.

NP injections within 2 hours of injury had the greatest preservation of motor function at 1 wpi relative to all other conditions, with retention of this increased function through day 42. Inflammatory cytokines and reactive oxygen species released by pro-inflammatory neutrophils and macrophages after SCI are cytotoxic towards neuronal cells [131,132]. IL-1α and TNFα in the injury microenvironment induce increased trafficking of glutamate receptors to neuron cell membranes and thereby cause increased excitotoxicity [16,17]. NP administration is able to alter the immune cell accumulation and polarization normally seen following SCI and contribute to the increased function by increasing sparing of neurons and motor circuits. Previous studies with NP injection

had been performed with a thoracic injury, and BMS scores for NP treated were increased relative to control mice by day 7 [76]. For the study herein that had a cervical injury, an increased functional response was again observed as early as day 7 for mice receiving particles at 2 hpi relative to control. At 1 wpi, all NP-treated mice, regardless of the timing for initial NP administration, had a larger number of surviving neurons contralateral to the injury than mice that did not receive NPs. Mice that received NPs starting at 24 hpi had fewer intact NMJs than even control mice receiving PBS injections at 2 hpi. These results suggest that even though neuron survival is not dependent upon time of first NP administration, early administration of NPs may maintain neuronal connections more effectively than later administration.

Mice with a spinal cord injury that received NPs at 4 hpi or later initially had motor performance similar to control mice, yet their motor performance improved over time. While unchecked immune response after SCI can lead to neuron cell death and axonal dieback, an attenuated inflammatory response can have reduced damage, such as demyelination of nerve fibers without axonal death, which leads to decreases in their conductive potential and functional deficits [133,134]. After the acute phase of injury, the surviving nerve fibers may have conduction recover partially or completely [134]. For the mice receiving particles at 4 hpi, we hypothesize that the initial deficit and gradual improvement may be associated with recovery from the conduction block. These mice had greater neuronal and NMJ sparing than mice that receive NPs at later times; thus, the recovery in function that was observed during subacute and chronic phases may reflect partial recovery in conduction in the spared motor circuits. Within the mice receiving NPs at 24 hpi, we anticipate that the recovery of function was associated with this recovery in the conduction of spared circuits. However, the initial immune response decreased the extent of spared NMJs relative to NPs delivered at earlier times, and thus the extent of recovery was more modest.

In conclusion, this report demonstrates that NP treatment can modulate the inflammatory microenvironment after SCI, and that NP administration within 24 hours is associated with a greater recovery of function relative to control. While the numbers of infiltrating immune cells are similar in NP-treated and control mice 2 days post-injury, fewer cells were present by the end of the first week post-injury. In addition to altering the immune microenvironment in the spinal cord, NP administration leads to increased sparing of neurons. Nevertheless, early administration of NPs is able to substantially attenuate the early functional deficits. Administration of NPs at later time points is associated with early functional deficits, yet these functional deficits improve with time, with greater levels of improvement with earlier timing of NP administration. These NPs may provide a therapeutic option for patients with SCI to limit secondary damage, as they are formed from a material that has been approved by the FDA for use in other indications, and is stable and could be available off-the-shelf.

Chapter 3 Nanoparticle and Epothilone D Combinatorial Intervention Improves Motor Performance and Regeneration in Chronic Cervical Spinal Cord Injury

3.1 Authors

Sarah E. Hocevar, Brian C. Ross, Samantha R. Schwartz, Brooke M. Smiley, Brain J. Cummings, Aileen J. Anderson, Lonnie D. Shea

3.2 Abstract

Spinal cord injury (SCI) causes the loss of motor function below the site of injury due to neuron loss and severing of spinal tracts. Circulating myeloid cells that are recruited to the injury create an inflammatory microenvironment that exacerbates cell death. Fibroblasts and astrocytes migrate to the injury site and form scar tissue that inhibit regeneration of severed axons. To combat these issues, we proposed a combinatorial treatment in a chronic cervical hemisection model. First, we administered cargo-less poly(lactide-co-glycolide) (PLG) nanoparticles (NPs). These NPs are administered intravenously and are phagocytosed by circulating myeloid cells, decreasing their infiltration of the spinal cord and polarizing them towards a less-inflammatory phenotype. Second, four weeks after injury we resected the injury area and inserted a microporous, multichannel PLG scaffold to reduce scar tissue and provide a substrate for axon regrowth. Third, we administered epothilone D (epoD), a microtubule stabilizer to further decrease fibrotic scar formation and improve axon elongation. Both NP treatment and epoD treatment alone (in combination with PLG scaffold) improved motor performance, but together they maximally improved function. Underlying this improved performance, mice that received NPs or EpoD exhibited increased neuromuscular junction innervation, robust axon growth into

the bridge, and both oligodendrocyte and Schwann-cell myelination of regenerating axons. Together, these results suggest that a combinatorial treatment plan that targets both inflammation and growth-inhibitory factors can improve motor performance following SCI.

3.3 Introduction

Spinal cord injury (SCI) causes permanent loss of sensory and motor function below the level of injury due to neuron and oligodendrocyte death. A variety of factors exacerbate the injury and limit the regenerative capability of the spinal cord. First, the infiltration of myeloid cells and the cytokines that they secrete exacerbate cell death and create a pervasive inflammatory environment [108,109,129,135,136]. Second, fibroblasts and astrocytes migrate to the injury site and form scar tissue[20,137-139]. Third, low expression of regeneration associated genes in the CNS and the presence of myelin debris and scar tissue inhibit axonal regeneration by neurons[140-142]. To combat these issues, we proposed a combinatorial approach in a chronic model of a cervical hemisection injury.

A variety of approaches have been explored to combat these issues. To attenuate inflammation, the glucocorticoid methylprednisolone has been used clinically but is not recommended as standard-of-care due to its many negative side effects[33-35]. Antibody therapy against neutrophils and monocytes and their adhesion molecules has reduced the accumulation of myeloid cells in the spinal cord but does not always lead to increased recovery[11,110,143]. We have previously used intravenous cargo-less PLG NPs that are phagocytosed by circulating myeloid cells, redirecting them away from the spinal cord and polarizing them towards a more anti-inflammatory phenotype[76].

A variety of biomaterials and growth factors have been investigated to provide a more growth-permissive environment in the damaged spinal cord. Chondroitinase ABC (ChABC) is an

enzyme that degrades chondroitin sulfate proteoglycans (CSPGs), a key component of the SCI scar that inhibits axon regrowth. ChABC has been widely shown in numerous SCI models to promote axonal elongation and motor recovery, but it must be delivered to the spinal cord via multiple intrathecal injections due to its heat instability [144-148]. Paclitaxel is a microtubule stabilizer that is used commonly used for chemotherapy and has been shown to limit glial scar formation and promote axon elongation, but it does not have the ability to cross the blood-spinal cord barrier [80-82]. Therefore, there exists a need for a systemically administered pharmacological agent that can attenuate scar formation and promote a growth-permissive environment. Epothilones are a class of FDA-approved microtubule-stabilizing agents that have been previously approved for use in triple-negative breast cancer and have the ability to cross the blood-spinal cord barrier [87-89]. Epothilones B and D have been shown to decrease scar formation and increase axon elongation following SCI, but their ability to enhance motor recovery remains unclear [90-93].

In this study we proposed a combinatorial approach to address both the inflammation and lack of neural regeneration following injury. We used a chronic cervical hemisection model wherein mice receive a lateral C5 hemisection and 4 weeks later we resected the injury area and implanted a biomaterial bridge. First, to combat the inflammation following injury, we administered cargo-less poly(lactide-co-glycolide) (PLG) nanoparticles (NPs). NPs are injected intravenously following injury and are phagocytosed by circulating monocytes and neutrophils [130], decreasing their migration to the SCI and reprogramming them towards an anti-inflammatory phenotype. Mice that received NP treatment made fewer mistakes on a ladder beam test of motor performance. Second, four weeks after injury, we resected scar tissue and inserted a microporous, multichannel PLG bridge. This removes inhibitory astroglial scar tissue and

provides a scaffold to guide regenerating axons across the injury site. We tested whether NP administration after the resection surgery can have a further beneficial effect. Mice that received NPs after both the initial injury and resection performed better on the ladder beam test than mice that received vehicle or NPs after only one surgery. Lastly, we administered epothilone D (epoD), a microtubule stabilizer that can penetrate the blood-brain barrier, to limit axon retraction and boost elongation. Mice received two doses of epoD, the first after the resection surgery, and the second two weeks post-resection. Groups that received epoD had reduced glial and fibrotic scarring. Additionally, epoD groups had greater neuromuscular junction (NMJ) innervation compared to groups that did not. Mice that received epoD performed better on the ladder beam task, and mice that received both epoD and NPs after both surgeries performed the best out of all groups. Underlying this performance, all mice that received NPs or epoD exhibited robust axon growth into the injury and both oligodendrocyte and Schwann cell myelination of regenerating axons. Together, these results suggest that a combinatorial treatment plan that targets both inflammation and growth-inhibitory factors can improve motor performance following SCI.

3.4 Methods

Multichannel PLG bridge production

Multichannel bridges were fabricated as previously described using a gas foaming technique to fuse PLG microparticles into a microporous matrix. 63-107 um NaCl was used as a sacrificial mold for micropores to allow cell infiltration and nine 150-250 um pulled sugar strands were used as a mold for channels that guide nerve growth.

NP production

50:50 PLG (inherent viscosity = 0.55dL/g; Evonik, Sand Creek, MI) was dissolved in dichloromethane and sonicated with a Cole-Parmer CPX130 Ultrasonic Processor (Vernon Hills, IL) to produce NPs. The mixture was stirred overnight to evaporate the organic phase and NPs were washed to remove excess PEMA. The particle size and charge were measured with a Zetasizer Nano ZSP (Malvern Panalytical, Malvern, United Kingdom) and the resulting NPs were 500-650 nm in diameter with a charge of approximately -40 mV. The particles were lyophilized with sucrose and D-mannitol (Sigma-Aldrich, St. Louis, MO) for storage.

Animal care and chronic cervical injury model

All animal work was done in concordance with guidelines by the Institutional Animal Care and Use Committee (IACUC) at the University of Michigan. A C5 lateral hemisection was performed on 6-8 week old male and female Crym-RFP (cross between Mutant Mouse Resource & Research Center #036627-UCD and Jackson Laboratory #007905) mice as previously described [149]. Briefly, mice were anesthetized with 2% isoflurane and 1 mg/kg bupivacaine was administered as a local anesthetic. A C5 laminectomy was performed and two lateral cuts were made above and below C5. The lateral cuts were made from midline to lateral using a microfeather scalpel. The injury and exposed spinal cord were covered in Gelfoam (Ethicon, Raritan, NJ). Muscles were sutured using 5/0 Chromic Gut (Henry Schein, Melville, NY), and the skin was stapled. Post-operative care consisted of buprenorphine (0.1 mg/kg) twice daily for 3 days, enrofloxacin (2.5 mg/kg, Bayer, Leverkusen, Germany) daily for 14 days, and lactated ringers' solution (1 mL, MWI Veterinary Supply, Boise, ID) daily for 5 days. Bladders were expressed twice daily until function recovered and wound clips were removed 10 days after surgery. Four weeks following the initial injury, the injury area was resected by connecting the

two lateral cuts vertically along the midline and a PLG bridge was implanted. Gelfoam was placed over the injury and spinal cord and post-operative care was performed as described above.

NP and EpoD administration

Mice received 1 mg PLG NPs suspended in 0.1 mL DPBS daily for one week following initial injury and resection surgery by lateral tail vein injection. NPs were first delivered within two hours of injury. Mice were given two doses of 1.5 mg/kg epoD (Cayman Chemicals) in DMSO by intraperitoneal injection: the first immediately following the second surgery and the second 14 days later.

Motor function assessment

A horizontal ladder beam test was conducted at 1-, 2-, 4-, 5-, 6-, 8-, 10-, 12-, 14-, and 16-weeks post-injury. As previously described, mice were trained on the ladder beam consisting of 50 rungs during the week prior to injury. Videos were scored by two blinded observers for 3 trials per animal by counting the number of correct and misplaced steps of the left forepaw on the ladder beam.

Immunohistochemistry

Mice were euthanized with 5% isoflurane and decapitation. Spinal cords were harvested at 4 weeks post-surgery to assess scar tissue formation and at 12 weeks post-surgery to assess axon regeneration. Briefly, C4-C7 were dissected and flash frozen with isopentane. Spinal cords were mounted in OCT medium with 30% sucrose and sectioned either longitudinally or transversely at a 14 um thickness. The left acromiotrapezius and left forearm flexor muscles were harvested at 12 weeks post-surgery to assess neuromuscular junction innervation and were cryosectioned longitudinally at 14 um thickness. Tissues were fixed with 4% paraformaldehyde, permeabilized with in 0.5% Triton in Tris-buffered saline, and blocked in donkey or goat serum as necessary.

The primary antibodies used were: chicken anti-NF200 (1:250, AVES Labs, Davis, CA, #NFH) for neurofilament, anti-bungarotoxin conjugated to Alexa Fluor 647 (1:500, Thermo Fisher, Waltham, MA, #B35450) for motor endplates, rabbit anti-neurofilament 200 (1:200, Sigma, #N4142), rat anti-MBP (1:200, Biorad, MCA409S) for myelination, and chicken anti-myelin protein zero (1:250 Aves labs, #PZ0) for Schwann cell myelination. Secondary antibodies were AlexaFluor 555 goat anti-rat (1:1000; Invitrogen #A21434), AlexaFluor 555 goat anti-mouse (1:1000; Invitrogen #A21424), and AlexaFluor 488 goat anti-chicken (1:1000; Invitrogen #A11039), AlexaFluor 488 goat anti-rabbit (1:1000, Invitrogen #A11008), and AlexaFluor 633 donkey anti-chicken (1:1000, Sigma, #SAB4600127). Tissues were imaged on an Axio Observer Z1 using an ORCA-Flash 4.0 V2 Digital CMOS camera. Images were quantified

IHC image quantification

To quantify regrowing axons in the SCI, a binary mask of the bridge area was made using Fiji. Tiff files were uploaded to Ilastik and pixel classification was performed after training a set of 4 randomly selected tissues per condition. Ilastik was trained using a single operator to ensure consistent training and the program was trained against a no-primary control to prevent non-specific training. The Ilastik output files were loaded into Cellprofiler along with the binary masks of the injury area. Only axons in the injury area were counted. Myelination was identified as colocalization of MBP with NF200 and Schwann cell myelination was identified as colocalization of Pzero with MBP and NF200. To quantify fibrotic and astrocytic scar formation, images were first cropped to a 2800 um x 2000 um area centered around the injury using Fiji. Area of scarring was determined by thresholding the images. To quantify NMJ innervation, tiff images were uploaded to Ilastik and image training was performed similarly as previously

described. The Ilastik output files were loaded into Cellprofiler and both motor endplates and innervated NMJs, defined as colocalization of NF200 with bungarotoxin, were quantified.

Statistical analysis

Statistical analysis was performed using Graphpad Prism 10. For immunohistochemistry n=5-8 mice were used per condition and values were analyzed using an ordinary one-way ANOVA with Tukey's post-hoc test. For ladder beam behavior data, n=8-10 mice were used per condition and values were analyzed using an ordinary one-way ANOVA with Tukey's post-hoc test.

3.5 Results

3.5.1 Nanoparticles improve motor function after chronic cervical injury

We have previously reported that NP treatment improves motor function in an acute spinal cord injury [76]. Therefore, we wanted to investigate whether NP treatment provides beneficial effects in a chronic model of SCI. Mice that received NPs after the initial injury trended towards a greater number of correct placements and fewer mistakes than control mice (Figure 3.1 A-B). At day 35 after the injury resection and bridge placement, control mice had significantly fewer correct placements ($p=0.022$) and more mistakes ($p=0.036$) (Figure 3.1C-D) than NP mice. At day 112 both NP and control mice showed improved motor recovery, but NP still had significantly greater correct placements ($p=0.0255$).

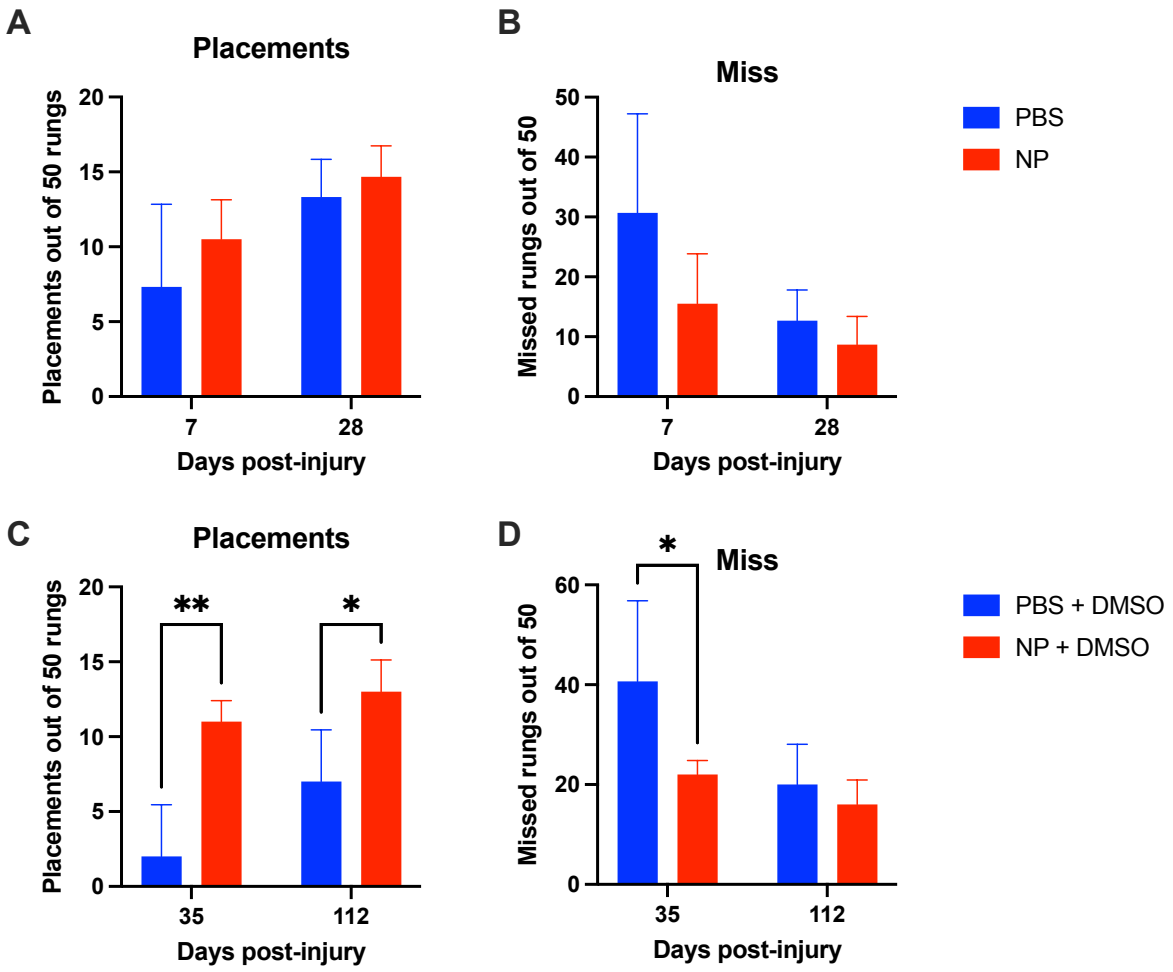


Figure 3.1 Ladder beam performance in chronic injury model after NP administration. The horizontal ladder beam test was performed biweekly following injury. The number of correct placements (A,C) and incorrect placements (B,D) were counted out of 50 rungs after injury (A,B) and following bridge implantation (C,D). Data are mean ± SD. n = 8-12 mice per condition. * $p < 0.05$, ** $p < 0.01$

3.5.2 Epothilone D reduces scar tissue formation

We next wanted to investigate whether NP treatment can synergize with other SCI treatments that promote regeneration, so we tested combinatorial treatment with EpoD. Mice received two doses of EpoD: the first dose was immediately following resection surgery, and the second dose was two weeks post-surgery. Mice that did not receive EpoD instead received DMSO as a vehicle control. Additionally, we wanted to test whether NP treatment could be beneficial when given after only the initial injury or bridge implantation. Therefore, we tested two additional

conditions: PBS first, NP second received PBS injections after the initial injury but NPs after the bridge implantation, and NP first, PBS second received the opposite. At 4 weeks post-surgery, mice that received NPs without EpoD did not have significantly different area of scar tissue formation compared with control PBS+DMSO mice (Figure 3.2A-C). However, mice that received EpoD with or without NPs had significantly lower fibronectin and GFAP scar tissue formation (Fibronectin: PBS+DMSO vs PBS+epo p=0.0008, NP+DMSO vs PBS+epo p=0.0031. GFAP: PBS+DMSO vs PBS+epo p=0.0229, NP+DMSO vs PBS+epo p =0.0007, NP+epo vs NP+DMSO p =0.0033). Collectively, these results show that EpoD has the ability to reduce both fibrotic and glial scar formation.

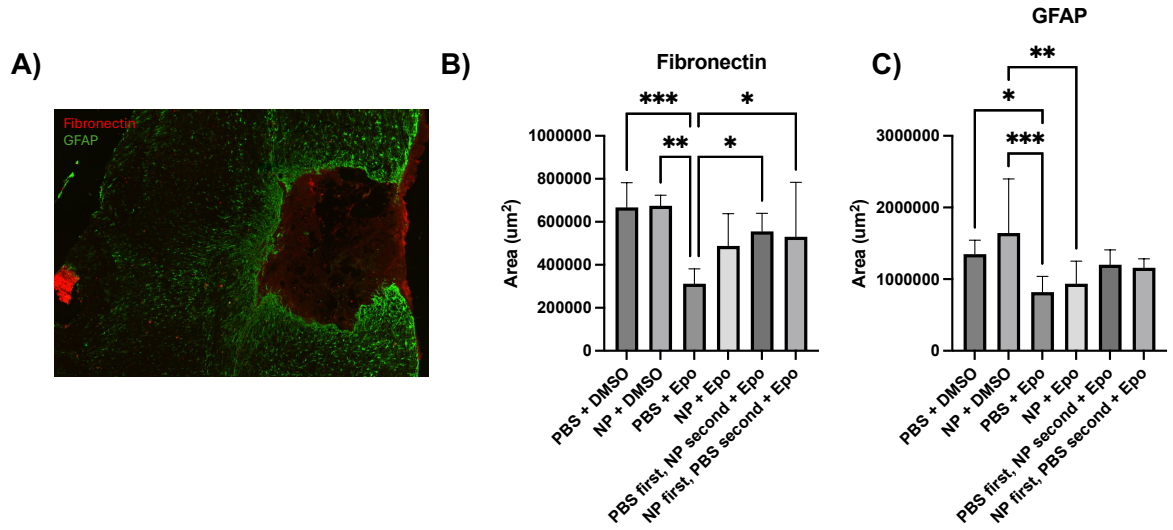


Figure 3.2 Fibrotic and glial scarring at 4 weeks post-bridge implantation. Spinal cords were harvested 4 weeks post-bridge implantation. A) Representative image of glial and fibrotic scarring. B) EpoD reduces fibrotic scar tissue area. C) EpoD also reduces astrocytic scar formation. Data are mean ± SD. n=6 mice per condition. *p<0.05 **p<0.01 ***p<0.001

3.5.3 Epothilone D improves axon regeneration

At 12 weeks post-bridge implantation, all conditions had robust axon growth into the PLG bridge (Figure 3.3A-B). NPs and EpoD did not have a significant impact on number of axons in the bridge. Mice that received both NPs and EpoD had greater oligodendrocyte myelination than

mice that did not receive EpoD (PBS+DMSO vs NP+epo p=0.0154, NP+DMSO vs NP+epo p = 0.0324) (Figure 3.3C). Neither NP nor EpoD treatment had a significant effect on myelination by Schwann cells.

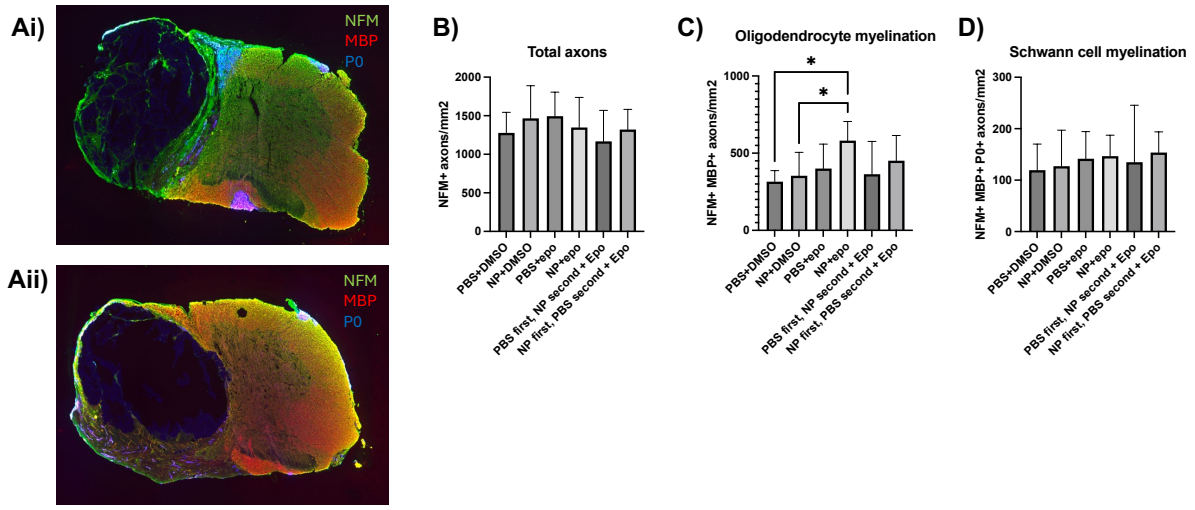


Figure 3.3 Axon growth and myelination into injury site at 12 weeks post-bridge implantation. Representative images of PBS+epo spinal cord (Ai) and NP+epo spinal cords (Aii). Total axons (B), axons myelinated by oligodendrocytes (C) and Schwann cells (D) were quantified by IHC. Data are mean ± SD. n=5-6 mice per condition. *p<0.05

3.5.4 Epothilone D improves NMJ innervation in chronic injury

Next, we investigated whether NPs and EpoD can improve neuromuscular junction innervation. Epothilone B has been shown to improve peripheral nerve regeneration, so we hypothesize that EpoD may help preserve or regenerate NMJs [150]. The acromiotrapezius (LA) and flexor carpi ulnaris and flexor digitorum profundus (LF) were harvested 12 weeks following resection surgery. NPs alone did not have a significant effect on motor endplate retention or NMJ innervation. EpoD whether alone or with NPs did significantly improve motor endplate sparing in the flexor muscles (Figures 3.4B) (PBS+DMSO vs PBS+epo p < 0.0001, PBS+DMSO vs NP+epo p = 0.0167). EpoD with and without NPs also significantly improved the percentage of innervated NMJs in both the ATZ (PBS+DMSO vs NP+epo p = 0.0021, NP+DMSO vs NP+epo p =0.0044) and flexor muscles (PBS+DMSO vs PBS+epo p < 0.0001, PBS+DMSO vs NP+epo p

< 0.0001, NP+DMSO vs NP+epo p < 0.0001) (Figures 3.4C-D). Collectively, EpoD with and without NP treatment has the ability to improve NMJ innervation.

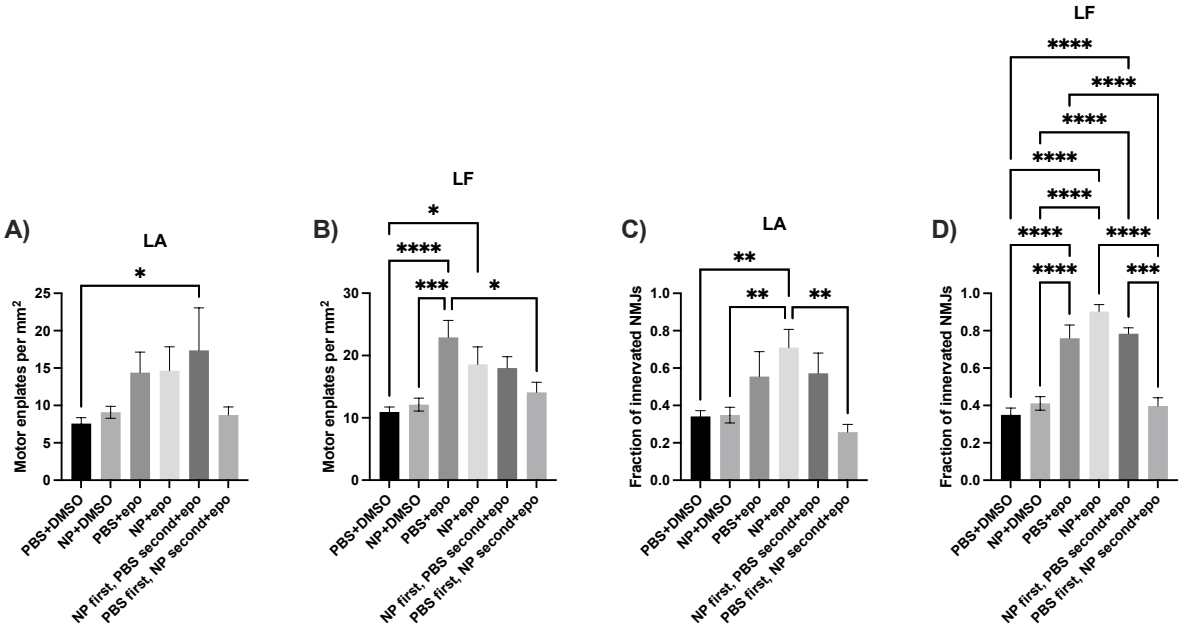


Figure 3.4 Neuromuscular junction innervation at 12 weeks post-bridge implantation. The acromiotrapezius (A, C) and flexor digitorum profundus and flexor carpi ulnaris (B,D) were harvested 12 weeks after bridge implantation. Motor endplates (A,B) and innervated NMJs (C,D) were quantified by IHC. Data are mean ±SD. n=5-8 mice per condition. *p<0.05 **p<0.01 ***p<0.001

3.5.5 Nanoparticle and epothilone D combinatorial treatment enhances motor recovery

Lastly, because EpoD improves axonal regeneration and NMJ innervation, we investigated whether it could enhance the motor recovery we see with NPs alone. At day 35, 7 days post-resection surgery, mice that received both NPs and EpoD had significantly fewer mistakes than mice that received only EpoD or received NPs only after the second surgery (NP+epo vs PBS+epo p = 0.0139, NP+epo vs PBS first, NP second p = 0.0145) (Figure 3.5B). By day 112, mice that received NPs and EpoD had significantly greater placements (p=0.0358) and fewer mistakes than mice that only received NPs after the second surgery (0.014) (Figure 3.5A-B). This shows that NPs and EpoD can synergistically improve motor recovery following chronic

injury and that there is a benefit to NP treatment after both the initial injury and resection surgery.

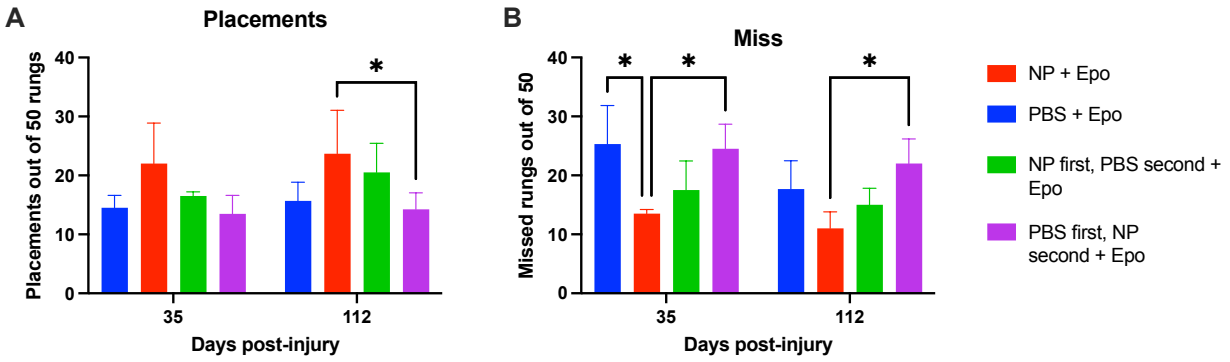


Figure 3.5 EpoD enhances motor function recovery in chronic injury after bridge implantation. The horizontal ladder beam test was performed biweekly following injury. The number of correct placements (A) and incorrect placements (B) were counted out of 50 rungs. Data are mean ±SD. n = 8-12 mice per condition. * $p < 0.05$

3.6 Discussion

In this study we investigated the utility of NP and EpoD therapy in a chronic cervical SCI model. Following SCI, circulating innate immune cells infiltrate the spinal cord and cause secondary damage. The resulting inflammation can exacerbate neuronal death, axonal degeneration and demyelination, and astroglial scar tissue formation. Ablation of neutrophils and monocytes paradoxically worsens functional outcomes [110]. While the glial scar inhibits axon growth, it is necessary to contain inflammatory cells and cytokines away from healthy tissue. Conditional ablation of astrocytes following mouse SCI has been found to lead to spread of inflammation, increased neuron loss, and worse functional outcomes [24,151,152]. Therefore, there exists a need for a therapy that modulates the immune and astrocytic responses rather than ablate them and promotes the formation of growth-permissive environment.

The NPs used in this study are phagocytosed by circulating immune cells and alter their trafficking and phenotype to promote a less inflammatory and pro-regenerative environment in the spinal cord. We have previously shown that these NPs can improve motor recovery and

axonal growth into the injury area after an acute injury [76]. Although the concentration of infiltrating immune cells peaks during the first week post-injury, macrophages and microglia remain in the spinal cord for months following injury and form part of the glial scar [128,153]. Therefore, we wanted to investigate the therapeutic efficacy of NPs in a chronic SCI model. NPs alone improved performance on a ladder beam test after chronic injury and bridge implantation. Mice that received NPs made fewer mistakes one week after bridge implantation and made more correct placements at both one and twelve weeks after implantation. The mechanisms underlying this improvement are not clear. There is no significant change in NMJ innervation of forelimb muscles, scar tissue formation, or axon regrowth after NP treatment alone. The implant surgery likely introduces some inflammation to the spinal cord when the scar tissue is resected, and the NPs may be working in a similar manner to what we have seen in our acute injury model in **Chapter 3**.

Most functional improvement occurs during the first weeks and months following SCI due to remaining neuroplasticity [106]. There are few treatments that aim to improve regeneration during the chronic phase of SCI after the glial scar has formed and axons have degenerated. Epothilones are a class of microtubule stabilizers that show promise as a treatment for chronic SCI because of their ability to cross the blood-spinal cord barrier after intraperitoneal administration, inhibit fibroblast migration, and promote axon elongation [80,90,154-156]. In this study, we found that EpoD alone significantly reduces scar tissue formation but does not improve axon regrowth or myelination. In a mouse model of ALS, EpoD was able to increase lower motor neuron sparing and NMJ innervation [156]. In our injury model, EpoD alone also improved motor endplate sparing and NMJ innervation in forelimb muscles, which may underlie improvements in motor function compared to negative control mice.

In this study, we found that mice that received both NPs and EpoD treatment had the greatest amount of motor function recovery of any experimental group. These mice that received combinatorial treatment had the greatest amount of NMJ innervation and motor endplate sparing. Receiving NPs after both the initial injury and the bridge implantation yielded the best motor results, but receiving NPs only after the initial injury plus EPO trended towards better function and NMJ innervation than mice that received EpoD alone. This further suggests that the NPs are primarily working by increasing tissue sparing by attenuating inflammation. Interestingly, mice that received both NPs and EpoD had greater fibrotic scarring than mice that received EpoD alone, but this did not detrimentally affect axon growth into the bridge or myelination of these axons. In fact, NPs and EpoD together produced the greatest amount of myelination in regenerating axons, which may be an indicator of better oligodendrocyte sparing from inflammation-induced apoptosis [157].

In conclusion, this study demonstrates that NP treatment can successfully modulate the inflammatory response in a chronic injury model to promote functional motor recovery. When combined with the microtubule stabilizer EpoD scar tissue reduction, myelination of regenerating axons, and motor recovery are further enhanced. This supports the need for a combinatorial treatment that can both reduce inflammatory secondary damage in the acute stage and promote a growth-permissive environment in the chronic stage of injury.

Chapter 4 Conclusions and Future Directions

4.1 Summary of Findings

Collectively, the work in this dissertation demonstrates the ability of cargo-less, PLG nanoparticles to reduce immune cell infiltration to the injured spinal cord and improve motor function. Following an acute C5 hemisection, we investigated the time window in which NP administration can modulate the immune response and increase functional sparing. We found that both early and delayed NP administration can improve neuron survival and motor function compared to controls. However, earlier administration best reduces immune cell infiltration into the spinal cord and promotes a higher level of motor function sparing than later administration timepoints. We also investigated the use of PLG NPs in a chronic cervical hemisection model. We found that NPs are able to increase motor function recovery in the chronic injury model. When combined with EpoD treatment, there was reduced scar tissue formation, increased oligodendrocyte myelination in regenerating axons, and increased motor recovery. The work presented in this dissertation builds upon previous work in our lab investigating SCI and advances our knowledge of how NPs influence immune cell trafficking to the injured spinal cord and motor function recovery.

4.2 Significance and Impact

Over 17,000 cases of SCI occur every year in the United States with the majority injuries being at the cervical level and occurring in male patients [1]. The majority of studies investigating SCI use a thoracic level contusion or compression injury and involve only female rodents [158-160]. While contusion and compression injuries are more common, patients with penetrating injuries

experience little spontaneous recovery after injury and there are no clinical therapies designed to reconnect severed spinal cord tracts[105,106]. Additionally, there are no standard-of-care treatments that address the inflammation and subsequent secondary damage after SCI. Therefore, the work presented in this dissertation addresses an unmet clinical need in SCI treatment.

In **Chapter 3**, we investigated how the timing of NP administration influences immune cell dynamics and motor function sparing. Our lab has previously published that delivering NPs within 2 hours of injury reduces macrophage and neutrophil infiltration into the SCI and improves motor function sparing in a thoracic hemisection model [76]. However, delivering NPs within 2 hours of injury in a clinical setting may be infeasible due to time constraints. Studies with methylprednisolone showed improved functional outcomes if administered within 8 hours of injury, which suggests that there may be a wider window of time in which immunomodulation can be effective for preserving function [161]. We found that early NP administration within 2 hours of injury provides the greatest sparing of motor function, later NP administration still improves motor function above control and all NP administration times lead to increased neuron sparing.

During the chronic phase of SCI, axon regrowth is hindered by the presence of fibrotic and glial scar tissue. In **Chapter 4**, we investigated the use of NPs in combination with EpoD in a chronic cervical SCI model. We found that when scar tissue is resected and a PLG bridge is implanted in a second surgery, both NPs and EpoD improve motor function and NMJ innervation in affected muscles. EpoD alone can decrease both glial and fibrotic scar formation, and EpoD in combination with NPs increases oligodendrocyte myelination of axons regrowing into the injury site. This chapter demonstrates the ability of NPs and EpoD to improve functional

outcomes in an injury model that normally exhibits little recovery and further demonstrates the clinical translatability of the NPs.

4.3 Future Directions

4.3.1 Investigation of Immune Cell Phenotype

The studies presented in this dissertation investigated the use of NPs for modulating the immune cell response following acute and chronic models of SCI. However, in these studies only the immune cell type was quantified. Both neutrophils and monocyte-derived macrophages can be polarized towards pro-inflammatory or anti-inflammatory phenotypes [162,163]. During normal wound healing, macrophages transition from a pro-inflammatory M1 phenotype towards a pro-regenerative M2 phenotype as healing progresses. This phenotype switch is delayed after SCI and prolongs secondary damage due to inflammation [112,128]. Therefore, it would be useful to understand whether NPs influence the phenotype of macrophages that accumulate after SCI to better understand how they contribute to neuron sparing and motor function recovery. The phenotype of immune cells could be investigated through flow cytometry using antibodies for M1 and M2 surface markers or through single cell RNA sequencing to determine the gene expression of immune cells in the injury[12,164,165].

4.3.2 Effects of NPs on astrocytes and endothelial cells

The blood-spinal cord barrier is the interface between the spinal cord and the vascular system and formed by astrocytic end feet, endothelial cells, and pericytes. Disruption of the blood-spinal cord barrier following SCI contributes to immune cell infiltration and the establishment of an inflammatory microenvironment [166-168]. In addition to physically disrupting the barrier, SCI causes changes in protein expression that contribute to immune cell accumulation and worse functional outcomes including decreasing aquaporin-4 expression, increased endothelin-1

expression, increased heme-oxygenase-1 expression [169-171]. Understanding the changes in gene expression in astrocytes and endothelial cells following SCI and NP treatment could help elucidate the mechanisms in which NP treatment reduces immune cell infiltration. Gene expression in astrocytes and endothelial cells could be investigated using single cell or single nuclei sequencing[168]. Blood-spinal cord barrier permeability can be assessed through contrast-enhanced MRI or the intravenous injection of tracer dyes such as cadaverine and subsequent spinal cord histology[172,173].

4.3.3 Nanoparticle design

This dissertation demonstrates that cargo-less PLG NPs made using PEMA as a surfactant can modulate the immune response following both acute and chronic SCI. The size, charge, and surface adsorption of proteins can affect the internalization of NPs by immune cells. Larger particles, charged particles and particles with adsorbed proteins are more readily internalized by immune cells than particles less than 200 nm, neutral particles, or adsorption-resistant particles [174-176]. Investigating design parameters of NPs could allow for engineering of NPs to target specific desired cell types and alter their phenotype and trafficking to achieve desired outcomes.

4.3.4 Other models of SCI

The studies in this dissertation use a penetrating model of SCI, but the majority of human SCI cases are contusion or compression injuries. Additionally, this dissertation only uses a mouse model of SCI. While mice experience inflammatory damage, scar tissue formation, and paralysis as humans do after SCI, the rat spinal cord behaves more similarly to human. Neutrophils infiltrate the spinal cord around 6 hours post-injury in both rats and mice, but neutrophil infiltration in mice can persist until two weeks post-injury whereas it declines in rats after 2 days [158,177]. Additionally, the injury site in mice forms a dense, fibrous core whereas in rats and

humans a cystic cavity forms at the center of the injury [178]. Investigating the use of NPs in models of SCI that are more relevant to human SCI and verifying their efficacy in these models will enhance the translatability of NP treatment.

Appendix

Appendix A: Adoptive Transfer of Myeloid Cells to Study the Effects of Nanoparticles on Immune Cell Infiltration in Spinal Cord Injury

Authors

Sarah E. Hocevar, Kate V. Griffin, Michael N. Saunders, Brian C. Ross, Samantha R. Schwartz, Brooke M. Smiley, Brain J. Cummings, Aileen J. Anderson, Lonnie D. Shea

Introduction

We have previously shown that NPs alter the accumulation of immune cells in the spinal cord after both acute and chronic spinal cord injuries [76]. In these studies, NPs were injected intravenously for one week following injury. Because these NPs are injected systemically, it is unknown whether they primarily work by directly associating with circulating immune cells and altering their trafficking or if there are other indirect factors that alter their accumulation in the spinal cord. In this study to separate the direct and indirect effects of the NPs on immune cell trafficking following SCI we conducted two separate adoptive transfer experiments. In the first experiment, bone marrow cells were harvested from naïve mice and incubated with NPs and CellTrace far red (CTFR) as a marker of adoptively transferred cells. The CTFR+ cells were then injected into mice with a C5 hemisection and flow cytometry was performed on the spinal cord the following day. There was a significantly lower percentage of NP+ adoptively transferred cells than NP- adoptively transferred cells, therefore showing that NPs directly alter the trafficking of myeloid cells. In the second experiment, to study the indirect effects of NPs on cell

trafficking, injured mice received intravenous NPs as previously described in **Chapters 2 and 3**. On day 3, CTFR+ bone marrow cells were adoptively transferred and flow cytometry performed on the spinal cord the next day. There was a significantly higher percentage of CTFR+ cells in mice that received only PBS compared to NPs, showing that NPs can also indirectly decrease the accumulation of immune cells in the spinal cord.

Methods

PLG and NP Fabrication

PLG bridges and NPs were made as previously described in **Chapter 3**.

Animal Handling and Spinal Cord Injury Model

The spinal cord injury and animal care were performed as previously described in **Chapter 3**.

Bone Marrow Isolation and Adoptive Transfer

Bone marrow was isolated from the femurs and tibias of uninjured 6-8-week-old female C57Bl/6 mice. The cell suspension was pooled and passes through a 70-um strainer with RPMI+glutamax (Gibco). Cells were spun down at 500g and red blood cells were lysed with ACK lysis buffer (Gibco) for 2 minutes. Cells were washed with media and spun down again. In the direct adoptive transfer experiment, cells were incubated with NPs for one hour and CellTrace Far-Red (Invitrogen) for 10 minutes. In the indirect experiment, cells were only incubated with CTFR Cells were washed and 2 million cells suspended in 0.2 mL DPBS (Gibco) were injected per recipient mouse.

Flow Cytometry

At 2 days post-injury spinal cord segments C4-C6 were harvested from recipient mice. Prior to flow cytometry, spinal cords were myelin depleted. Spinal cords were minced using spring

scissors (FST) and incubated with 0.5 mg trypsin (Millipore Sigma) and 1 mg collagenase (Millipore Sigma) in 3 mL DMEM (Gibco) per sample for 20 minutes in a 37 C incubator. Samples were placed on a rotisserie rocker to prevent the tissue from aggregating. After the incubation, the trypsin and collagenase were neutralized with DMEM + 10% FBS. The samples were spun down and resuspended in 480 uL of MACS buffer. The samples were demyelinated using the Miltenyi Myelin Removal Beads II kit with 20 uL of beads/sample. Following myelin depletion, cells were resuspended in MACS buffer and 1 million cells per sample were used for flow cytometry. Cells were incubated with Live/Dead Fixable Violet (Invitrogen) for 30 minutes on ice. Nonspecific antibody body was blocked by incubating with CD16/32 for 10 minutes on ice (Invitrogen). Samples were incubated with the following antibodies for 30 minutes on ice: Cd11b BV421 (0.25 ug/sample; Biolegend 101251), Ly6C BV510 (0.5 ug/sample; Biolegend 128033), and Ly6G PE (0.25 ug/sample; Biolegend 127608). Compensation samples were prepared by adding antibodies to AbC Antibody Compensation Beads (Invitrogen). Samples were resusupend in 100 uL MACs buffer before being run on a Biorad ZE5 Cell Analyzer. Data was analyzed using FlowJo (BD).

Statistical Analyses

Statistical analysis was performed using Graphpad Prism 10. For flow cytometry n=4-5 mice were used per condition and values were analyzed using an unpaired two-tailed t-test.

Preliminary Results

NPs directly reduce immune cell migration to the spinal cord

To study the direct effects of NP treatment on immune cell trafficking, bone marrow cells were incubated with NPs and CTFR prior to being adoptively transferred into injured mice. There

were significantly more NP- adoptively transferred CTFR+ cells in the spinal cord following injury than NP+ cells (p< <0.0001) (Figure 1A). Therefore, NPs have a direct effect on the immune cells to reduce their infiltration in the SCI. Of the adoptively transferred cells, there were significantly more NP+ Ly6C+ monocytes than NP- monocytes (Figure 1B), suggesting NPs may not redirect monocytes away from the SCI. There was no difference in the percentage of Ly6G+ neutrophils that were NP+ or NP- (Figure 1C).

Indirect effects of NPs on immune cell trafficking

To investigate the indirect effects of NPs on immune cell trafficking, mice received NP or PBS injections for 3 days prior to CTFR+ bone marrow cells being injected. There was a greater percentage of total CTFR+ adoptively transferred cells in mice that received PBS than NPs (Figure 2A) (p=0.0294). When further characterizing the CTFR+ cells in the spinal cord, there was no difference between NP and control in the percentage of CD11b+ myeloid cells (Figure 2B), Ly6C+ monocytes (Figure 2C), or Ly6G+ neutrophils (Figure 2D). Therefore, NPs have the capability to change the environment of the spinal cord such that they are indirectly decreasing the total immune cell trafficking to the injury, but they did not preferentially affect any specific myeloid cell type.

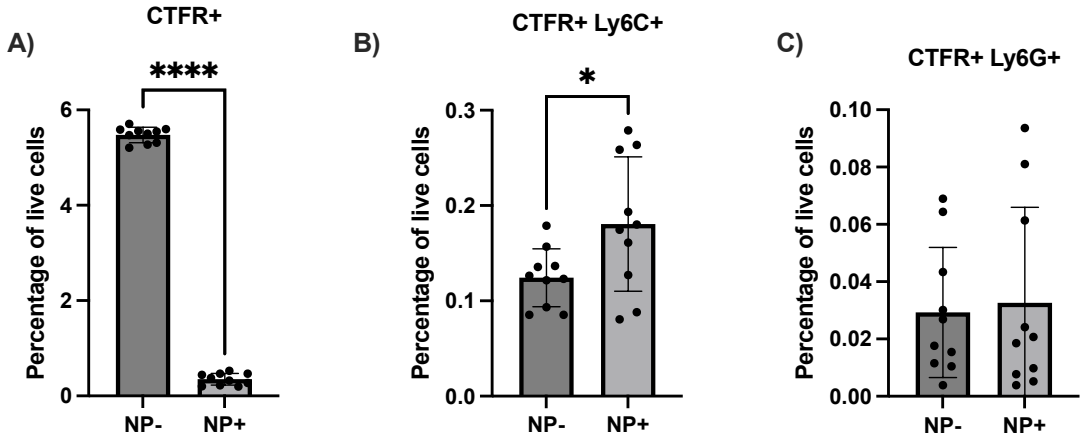


Figure A.1: Direct effects of NPs on immune cell trafficking. Flow cytometry for all adoptively transferred cells (A), adoptively transferred monocytes (b), and adoptively transferred neutrophils (c). Mean ± SD. *p<0.05, **** p<0.0001

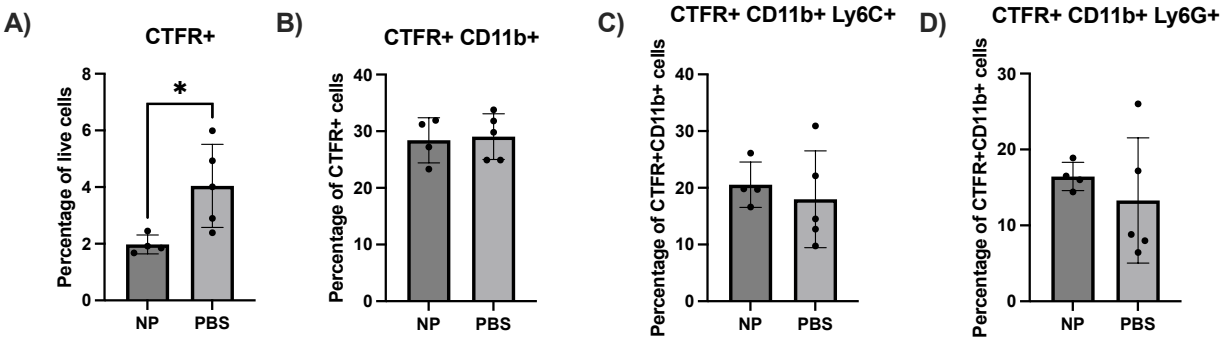


Figure A.2: Indirect effects of NPs on immune cell trafficking. Flow cytometry for all adoptively transferred cells (a), adoptively transferred myeloid cells (b), adoptively transferred monocytes (c), and adoptively transferred neutrophils (d). Mean ± SD. *p<0.05

Bibliography

1. Jain NB, Ayers GD, Peterson EN, et al. Traumatic spinal cord injury in the United States, 1993-2012. *Jama*. Jun 9 2015;313(22):2236-43. doi:10.1001/jama.2015.6250

2. Ma VY, Chan L, Carruthers KJ. Incidence, prevalence, costs, and impact on disability of common conditions requiring rehabilitation in the United States: stroke, spinal cord injury, traumatic brain injury, multiple sclerosis, osteoarthritis, rheumatoid arthritis, limb loss, and back pain. *Arch Phys Med Rehabil*. May 2014;95(5):986-995.e1. doi:10.1016/j.apmr.2013.10.032

3. Blair JA, Possley DR, Petfield JL, Schoenfeld AJ, Lehman RA, Hsu JR. Military penetrating spine injuries compared with blunt. *Spine J*. Sep 2012;12(9):762-8. doi:10.1016/j.spinee.2011.10.009

4. Bareyre FM, Kerschensteiner M, Raineteau O, Mettenleiter TC, Weinmann O, Schwab ME. The injured spinal cord spontaneously forms a new intraspinal circuit in adult rats. *Nat Neurosci*. Mar 2004;7(3):269-77. doi:10.1038/nn1195

5. Tuszynski MH, Steeves JD, Fawcett JW, et al. Guidelines for the conduct of clinical trials for spinal cord injury as developed by the ICCP Panel: clinical trial inclusion/exclusion criteria and ethics. *Spinal Cord*. Mar 2007;45(3):222-31. doi:10.1038/sj.sc.3102009

6. Oudega M, Perez MA. Corticospinal reorganization after spinal cord injury. *J Physiol*. Aug 15 2012;590(16):3647-63. doi:10.1113/jphysiol.2012.233189

7. Fouad K, Pedersen V, Schwab ME, Brösamle C. Cervical sprouting of corticospinal fibers after thoracic spinal cord injury accompanies shifts in evoked motor responses. *Curr Biol*. Nov 13 2001;11(22):1766-70. doi:10.1016/s0960-9822(01)00535-8

8. Rosenzweig ES, Courtine G, Jindrich DL, et al. Extensive spontaneous plasticity of corticospinal projections after primate spinal cord injury. *Nat Neurosci*. Dec 2010;13(12):1505-10. doi:10.1038/nn.2691

9. Rice T, Larsen J, Rivest S, Yong VW. Characterization of the early neuroinflammation after spinal cord injury in mice. *J Neuropathol Exp Neurol*. Mar 2007;66(3):184-95. doi:10.1097/01.jnen.0000248552.07338.7f

10. Alizadeh A, Dyck SM, Karimi-Abdolrezaee S. Traumatic Spinal Cord Injury: An Overview of Pathophysiology, Models and Acute Injury Mechanisms. *Front Neurol*. 2019;10:282. doi:10.3389/fneur.2019.00282

11. Lee SM, Rosen S, Weinstein P, van Rooijen N, Noble-Haeusslein LJ. Prevention of both neutrophil and monocyte recruitment promotes recovery after spinal cord injury. *J Neurotrauma*. Sep 2011;28(9):1893-907. doi:10.1089/neu.2011.1860

12. Beck KD, Nguyen HX, Galvan MD, Salazar DL, Woodruff TM, Anderson AJ. Quantitative analysis of cellular inflammation after traumatic spinal cord injury: evidence for a multiphasic inflammatory response in the acute to chronic environment. *Brain*. Feb 2010;133(Pt 2):433-47. doi:10.1093/brain/awp322

13. Hellenbrand DJ, Quinn CM, Piper ZJ, Morehouse CN, Fixel JA, Hanna AS. Inflammation after spinal cord injury: a review of the critical timeline of signaling cues and cellular infiltration. *J Neuroinflammation*. Dec 7 2021;18(1):284. doi:10.1186/s12974-021-02337-2

14. Anwar MA, Al Shehabi TS, Eid AH. Inflammogenesis of Secondary Spinal Cord Injury. *Front Cell Neurosci*. 2016;10:98. doi:10.3389/fncel.2016.00098

15. Mukhamedshina YO, Akhmetzyanova ER, Martynova EV, Khaiboullina SF, Galieva LR, Rizvanov AA. Systemic and Local Cytokine Profile following Spinal Cord Injury in Rats: A Multiplex Analysis. *Front Neurol*. 2017;8:581. doi:10.3389/fneur.2017.00581

16. Choi JI, Svensson CI, Koehrn FJ, Bhuskute A, Sorkin LS. Peripheral inflammation induces tumor necrosis factor dependent AMPA receptor trafficking and Akt phosphorylation in spinal cord in addition to pain behavior. *Pain*. May 2010;149(2):243-253. doi:10.1016/j.pain.2010.02.008

17. Zhang L, Berta T, Xu ZZ, Liu T, Park JY, Ji RR. TNF-α contributes to spinal cord synaptic plasticity and inflammatory pain: distinct role of TNF receptor subtypes 1 and 2. *Pain*. Feb 2011;152(2):419-427. doi:10.1016/j.pain.2010.11.014

18. Filbin MT. Myelin-associated inhibitors of axonal regeneration in the adult mammalian CNS. *Nat Rev Neurosci*. Sep 2003;4(9):703-13. doi:10.1038/nrn1195

19. Yiu G, He Z. Glial inhibition of CNS axon regeneration. *Nat Rev Neurosci*. Aug 2006;7(8):617-27. doi:10.1038/nrn1956

20. Ayazi M, Zivkovic S, Hammel G, Stefanovic B, Ren Y. Fibrotic Scar in CNS Injuries: From the Cellular Origins of Fibroblasts to the Molecular Processes of Fibrotic Scar Formation. *Cells*. Aug 2 2022;11(15)doi:10.3390/cells11152371

21. James G, Butt AM. P2Y and P2X purinoceptor mediated Ca2+ signalling in glial cell pathology in the central nervous system. *Eur J Pharmacol*. Jul 5 2002;447(2-3):247-60. doi:10.1016/s0014-2999(02)01756-9

22. Liddelow SA, Guttenplan KA, Clarke LE, et al. Neurotoxic reactive astrocytes are induced by activated microglia. *Nature*. Jan 26 2017;541(7638):481-487. doi:10.1038/nature21029

23. Wanner IB, Anderson MA, Song B, et al. Glial scar borders are formed by newly proliferated, elongated astrocytes that interact to corral inflammatory and fibrotic cells via STAT3-dependent mechanisms after spinal cord injury. *J Neurosci*. Jul 31 2013;33(31):12870-86. doi:10.1523/jneurosci.2121-13.2013

24. Yang T, Dai Y, Chen G, Cui S. Dissecting the Dual Role of the Glial Scar and Scar-Forming Astrocytes in Spinal Cord Injury. *Front Cell Neurosci*. 2020;14:78. doi:10.3389/fncel.2020.00078

25. Sofroniew MV. Astrocyte barriers to neurotoxic inflammation. *Nat Rev Neurosci*. May 2015;16(5):249-63. doi:10.1038/nrn3898

26. Smith-Thomas LC, Fok-Seang J, Stevens J, et al. An inhibitor of neurite outgrowth produced by astrocytes. *J Cell Sci*. Jun 1994;107 (Pt 6):1687-95. doi:10.1242/jcs.107.6.1687

27. Dou CL, Levine JM. Inhibition of neurite growth by the NG2 chondroitin sulfate proteoglycan. *J Neurosci*. Dec 1994;14(12):7616-28. doi:10.1523/jneurosci.14-12-07616.1994

28. Snow DM, Lemmon V, Carrino DA, Caplan AI, Silver J. Sulfated proteoglycans in astroglial barriers inhibit neurite outgrowth in vitro. *Exp Neurol*. Jul 1990;109(1):111-30. doi:10.1016/s0014-4886(05)80013-5

29. Tuinstra HM, Ducommun MM, Briley WE, Shea LD. Gene delivery to overcome astrocyte inhibition of axonal growth: an in vitro model of the glial scar. *Biotechnol Bioeng*. Mar 2013;110(3):947-57. doi:10.1002/bit.24750

30. Eckert MJ, Martin MJ. Trauma: Spinal Cord Injury. *Surg Clin North Am*. Oct 2017;97(5):1031-1045. doi:10.1016/j.suc.2017.06.008

31. Fehlings MG, Vaccaro A, Wilson JR, et al. Early versus delayed decompression for traumatic cervical spinal cord injury: results of the Surgical Timing in Acute Spinal Cord Injury Study (STASCIS). *PLoS One*. 2012;7(2):e32037. doi:10.1371/journal.pone.0032037

32. Jug M, Kejžar N, Vesel M, et al. Neurological Recovery after Traumatic Cervical Spinal Cord Injury Is Superior if Surgical Decompression and Instrumented Fusion Are Performed within 8 Hours versus 8 to 24 Hours after Injury: A Single Center Experience. *J Neurotrauma*. Sep 15 2015;32(18):1385-92. doi:10.1089/neu.2014.3767

33. Liu Z, Yang Y, He L, et al. High-dose methylprednisolone for acute traumatic spinal cord injury: A meta-analysis. *Neurology*. Aug 27 2019;93(9):e841-e850. doi:10.1212/wnl.0000000000007998

34. Rouanet C, Reges D, Rocha E, Gagliardi V, Silva GS. Traumatic spinal cord injury: current concepts and treatment update. *Arq Neuropsiquiatr*. Jun 2017;75(6):387-393. doi:10.1590/0004-282x20170048

35. Sámano C, Nistri A. Mechanism of Neuroprotection Against Experimental Spinal Cord Injury by Riluzole or Methylprednisolone. *Neurochem Res*. Jan 2019;44(1):200-213. doi:10.1007/s11064-017-2459-6

36. Duan R, Qu M, Yuan Y, et al. Clinical Benefit of Rehabilitation Training in Spinal Cord Injury: A Systematic Review and Meta-Analysis. *Spine (Phila Pa 1976)*. Mar 15 2021;46(6):E398-e410. doi:10.1097/brs.0000000000003789

37. Dietz V, Fouad K. Restoration of sensorimotor functions after spinal cord injury. *Brain*. Mar 2014;137(Pt 3):654-67. doi:10.1093/brain/awt262

38. Kapadia N, Masani K, Catharine Craven B, et al. A randomized trial of functional electrical stimulation for walking in incomplete spinal cord injury: Effects on walking competency. *J Spinal Cord Med*. Sep 2014;37(5):511-24. doi:10.1179/2045772314y.0000000263

39. Lorach H, Galvez A, Spagnolo V, et al. Walking naturally after spinal cord injury using a brain-spine interface. *Nature*. Jun 2023;618(7963):126-133. doi:10.1038/s41586-023-06094-5

40. Marquez-Chin C, Popovic MR. Functional electrical stimulation therapy for restoration of motor function after spinal cord injury and stroke: a review. *Biomed Eng Online*. May 24 2020;19(1):34. doi:10.1186/s12938-020-00773-4

41. Rejc E, Angeli CA, Atkinson D, Harkema SJ. Motor recovery after activity-based training with spinal cord epidural stimulation in a chronic motor complete paraplegic. *Sci Rep*. Oct 26 2017;7(1):13476. doi:10.1038/s41598-017-14003-w

42. Bracken MB, Shepard MJ, Holford TR, et al. Administration of methylprednisolone for 24 or 48 hours or tirilazad mesylate for 48 hours in the treatment of acute spinal cord injury. Results of the Third National Acute Spinal Cord Injury Randomized Controlled Trial. National Acute Spinal Cord Injury Study. *Jama*. May 28 1997;277(20):1597-604.

43. Dalal KL, Felix ER, Cardenas DD. Pregabalin for the management of neuropathic pain in spinal cord injury. *Pain Manag*. Sep 2013;3(5):359-67. doi:10.2217/pmt.13.35

44. de Sousa N, Santos D, Monteiro S, Silva N, Barreiro-Iglesias A, Salgado AJ. Role of Baclofen in Modulating Spasticity and Neuroprotection in Spinal Cord Injury. *J Neurotrauma*. Feb 2022;39(3-4):249-258. doi:10.1089/neu.2020.7591

45. Chen JY, Fu EJ, Patel PR, et al. Lentiviral Interleukin-10 Gene Therapy Preserves Fine Motor Circuitry and Function After a Cervical Spinal Cord Injury in Male and Female Mice. *Neurotherapeutics*. Jan 2021;18(1):503-514. doi:10.1007/s13311-020-00946-y

46. Smith DR, Dumont CM, Park J, et al. Polycistronic Delivery of IL-10 and NT-3 Promotes Oligodendrocyte Myelination and Functional Recovery in a Mouse Spinal Cord Injury Model. *Tissue Eng Part A*. Jun 2020;26(11-12):672-682. doi:10.1089/ten.TEA.2019.0321

47. Assinck P, Duncan GJ, Hilton BJ, Plemel JR, Tetzlaff W. Cell transplantation therapy for spinal cord injury. *Nat Neurosci*. Apr 25 2017;20(5):637-647. doi:10.1038/nn.4541

48. Gong Z, Xia K, Xu A, et al. Stem Cell Transplantation: A Promising Therapy for Spinal Cord Injury. *Curr Stem Cell Res Ther*. 2020;15(4):321-331. doi:10.2174/1574888x14666190823144424

49. Nandoe Tewarie RS, Hurtado A, Bartels RH, Grotenhuis A, Oudega M. Stem cell-based therapies for spinal cord injury. *J Spinal Cord Med*. 2009;32(2):105-14. doi:10.1080/10790268.2009.11760761

50. Kong XB, Tang QY, Chen XY, Tu Y, Sun SZ, Sun ZL. Polyethylene glycol as a promising synthetic material for repair of spinal cord injury. *Neural Regen Res*. Jun 2017;12(6):1003-1008. doi:10.4103/1673-5374.208597

51. Ross BC, Kent RN, 3rd, Saunders MN, et al. Building-Block Size Mediates Microporous Annealed Particle Hydrogel Tube Microenvironment Following Spinal Cord Injury. *Adv Healthc Mater*. Oct 2024;13(25):e2302498. doi:10.1002/adhm.202302498

52. Kushchayev SV, Giers MB, Hom Eng D, et al. Hyaluronic acid scaffold has a neuroprotective effect in hemisection spinal cord injury. *J Neurosurg Spine*. Jul 2016;25(1):114-24. doi:10.3171/2015.9.Spine15628

53. Menezes K, de Menezes JR, Nascimento MA, Santos Rde S, Coelho-Sampaio T. Polylaminin, a polymeric form of laminin, promotes regeneration after spinal cord injury. *Faseb j*. Nov 2010;24(11):4513-22. doi:10.1096/fj.10-157628

54. Raynald, Shu B, Liu XB, et al. Polypyrrole/polylactic acid nanofibrous scaffold cotransplanted with bone marrow stromal cells promotes the functional recovery of spinal cord injury in rats. *CNS Neurosci Ther*. Sep 2019;25(9):951-964. doi:10.1111/cns.13135

55. Saadinam F, Azami M, Pedram MS, et al. Injectable alginate chitosan hydrogel as a promising bioengineered therapy for acute spinal cord injury. *Sci Rep*. Nov 5 2024;14(1):26747. doi:10.1038/s41598-024-77995-2

56. Xiang W, Cao H, Tao H, et al. Applications of chitosan-based biomaterials: From preparation to spinal cord injury neuroprosthetic treatment. *Int J Biol Macromol*. Mar 1 2023;230:123447. doi:10.1016/j.ijbiomac.2023.123447

57. Suzuki H, Imajo Y, Funaba M, Ikeda H, Nishida N, Sakai T. Current Concepts of Biomaterial Scaffolds and Regenerative Therapy for Spinal Cord Injury. *Int J Mol Sci*. Jan 28 2023;24(3)doi:10.3390/ijms24032528

58. Feng C, Deng L, Yong YY, et al. The Application of Biomaterials in Spinal Cord Injury. *Int J Mol Sci*. Jan 3 2023;24(1)doi:10.3390/ijms24010816

59. Tuinstra HM, Margul DJ, Goodman AG, et al. Long-term characterization of axon regeneration and matrix changes using multiple channel bridges for spinal cord regeneration. *Tissue Eng Part A*. Mar 2014;20(5-6):1027-37. doi:10.1089/ten.TEA.2013.0111

60. Yang Y, De Laporte L, Zelivyanskaya ML, et al. Multiple channel bridges for spinal cord injury: cellular characterization of host response. *Tissue Eng Part A*. Nov 2009;15(11):3283-95. doi:10.1089/ten.TEA.2009.0081

61. Thomas AM, Kubilius MB, Holland SJ, et al. Channel density and porosity of degradable bridging scaffolds on axon growth after spinal injury. *Biomaterials*. Mar 2013;34(9):2213-20. doi:10.1016/j.biomaterials.2012.12.002

62. Nekanti U, Sakthivel PS, Zahedi A, et al. Multichannel bridges and NSC synergize to enhance axon regeneration, myelination, synaptic reconnection, and recovery after SCI. *NPJ Regen Med*. Mar 18 2024;9(1):12. doi:10.1038/s41536-024-00356-0

63. Dumont CM, Munsell MK, Carlson MA, Cummings BJ, Anderson AJ, Shea LD. Spinal Progenitor-Laden Bridges Support Earlier Axon Regeneration Following Spinal Cord Injury. *Tissue Eng Part A*. Nov 2018;24(21-22):1588-1602. doi:10.1089/ten.TEA.2018.0053

64. Park J, Decker JT, Margul DJ, et al. Local Immunomodulation with Anti-inflammatory Cytokine-Encoding Lentivirus Enhances Functional Recovery after Spinal Cord Injury. *Mol Ther*. Jul 5 2018;26(7):1756-1770. doi:10.1016/j.ymthe.2018.04.022

65. Chen TC, Mackic JB, McComb JG, Giannotta SL, Weiss MH, Zlokovic BV. Cellular uptake and transport of methylprednisolone at the blood-brain barrier. *Neurosurgery*. Feb 1996;38(2):348-54. doi:10.1097/00006123-199602000-00023

66. Fellner S, Bauer B, Miller DS, et al. Transport of paclitaxel (Taxol) across the blood-brain barrier in vitro and in vivo. *J Clin Invest*. Nov 2002;110(9):1309-18. doi:10.1172/jci15451

67. Chakraborty A, Ciciriello AJ, Dumont CM, Pearson RM. Nanoparticle-Based Delivery to Treat Spinal Cord Injury-a Mini-review. *AAPS PharmSciTech*. Mar 12 2021;22(3):101. doi:10.1208/s12249-021-01975-2

68. Yang Q, Lu D, Wu J, et al. Nanoparticles for the treatment of spinal cord injury. *Neural Regen Res*. Jun 1 2025;20(6):1665-1680. doi:10.4103/nrr.Nrr-d-23-01848

69. Kim JW, Mahapatra C, Hong JY, et al. Functional Recovery of Contused Spinal Cord in Rat with the Injection of Optimal-Dosed Cerium Oxide Nanoparticles. *Adv Sci (Weinh)*. Oct 2017;4(10):1700034. doi:10.1002/advs.201700034

70. Li L, Xiao B, Mu J, et al. A MnO(2) Nanoparticle-Dotted Hydrogel Promotes Spinal Cord Repair via Regulating Reactive Oxygen Species Microenvironment and Synergizing with Mesenchymal Stem Cells. *ACS Nano*. Dec 24 2019;13(12):14283-14293. doi:10.1021/acsnano.9b07598

71. Papastefanaki F, Jakovcevski I, Poulia N, et al. Intraspinal Delivery of Polyethylene Glycol-coated Gold Nanoparticles Promotes Functional Recovery After Spinal Cord Injury. *Mol Ther*. Jun 2015;23(6):993-1002. doi:10.1038/mt.2015.50

72. Wang D, Wang K, Liu Z, Wang Z, Wu H. Valproic acid-labeled chitosan nanoparticles promote recovery of neuronal injury after spinal cord injury. *Aging (Albany NY)*. May 28 2020;12(10):8953-8967. doi:10.18632/aging.103125

73. Azizi M, Farahmandghavi F, Joghataei MT, et al. ChABC-loaded PLGA nanoparticles: A comprehensive study on biocompatibility, functional recovery, and axonal regeneration in animal model of spinal cord injury. *Int J Pharm*. Mar 15 2020;577:119037. doi:10.1016/j.ijpharm.2020.119037

74. Jeong SJ, Cooper JG, Ifergan I, et al. Intravenous immune-modifying nanoparticles as a therapy for spinal cord injury in mice. *Neurobiol Dis*. Dec 2017;108:73-82. doi:10.1016/j.nbd.2017.08.006

75. Nukolova NV, Aleksashkin AD, Abakumova TO, et al. Multilayer polyion complex nanoformulations of superoxide dismutase 1 for acute spinal cord injury. *J Control Release*. Jan 28 2018;270:226-236. doi:10.1016/j.jconrel.2017.11.044

76. Park J, Zhang Y, Saito E, et al. Intravascular innate immune cells reprogrammed via intravenous nanoparticles to promote functional recovery after spinal cord injury. *Proc Natl Acad Sci U S A*. Jul 23 2019;116(30):14947-14954. doi:10.1073/pnas.1820276116

77. Blanquie O, Bradke F. Cytoskeleton dynamics in axon regeneration. *Curr Opin Neurobiol*. Aug 2018;51:60-69. doi:10.1016/j.conb.2018.02.024

78. Filous AR, Schwab JM. Determinants of Axon Growth, Plasticity, and Regeneration in the Context of Spinal Cord Injury. *Am J Pathol*. Jan 2018;188(1):53-62. doi:10.1016/j.ajpath.2017.09.005

79. Ertürk A, Hellal F, Enes J, Bradke F. Disorganized microtubules underlie the formation of retraction bulbs and the failure of axonal regeneration. *J Neurosci*. Aug 22 2007;27(34):9169-80. doi:10.1523/jneurosci.0612-07.2007

80. Hellal F, Hurtado A, Ruschel J, et al. Microtubule stabilization reduces scarring and causes axon regeneration after spinal cord injury. *Science*. Feb 18 2011;331(6019):928-31. doi:10.1126/science.1201148

81. Sengottuvel V, Leibinger M, Pfreimer M, Andreadaki A, Fischer D. Taxol facilitates axon regeneration in the mature CNS. *J Neurosci*. Feb 16 2011;31(7):2688-99. doi:10.1523/jneurosci.4885-10.2011

82. Nazemi Z, Nourbakhsh MS, Kiani S, et al. Co-delivery of minocycline and paclitaxel from injectable hydrogel for treatment of spinal cord injury. *J Control Release*. May 10 2020;321:145-158. doi:10.1016/j.jconrel.2020.02.009

83. Sun X, Xiong T, Yang K, et al. Individually Tailored Modular "Egg" Hydrogels Capable of Spatiotemporally Controlled Drug Release for Spinal Cord Injury Repair. *Adv Healthc Mater*. Oct 2023;12(27):e2301169. doi:10.1002/adhm.202301169

84. Zhang X, Xiong W, Kong G, et al. Paclitaxel-incorporated nanoparticles improve functional recovery after spinal cord injury. *Front Pharmacol*. 2022;13:957433. doi:10.3389/fphar.2022.957433

85. Zhu S, Wu Q, Ying Y, et al. Tissue-Adaptive BSA Hydrogel with Dual Release of PTX and bFGF Promotes Spinal Cord Injury Repair via Glial Scar Inhibition and Axon Regeneration. *Small*. Dec 2024;20(51):e2401407. doi:10.1002/smll.202401407

86. Goodin S. Novel cytotoxic agents: epothilones. *Am J Health Syst Pharm*. May 15 2008;65(10 Suppl 3):S10-5. doi:10.2146/ajhp080089

87. Villegas C, González-Chavarría I, Burgos V, Iturra-Beiza H, Ulrich H, Paz C. Epothilones as Natural Compounds for Novel Anticancer Drugs Development. *Int J Mol Sci*. Mar 23 2023;24(7)doi:10.3390/ijms24076063

88. Ballatore C, Brunden KR, Huryn DM, Trojanowski JQ, Lee VM, Smith AB, 3rd. Microtubule stabilizing agents as potential treatment for Alzheimer's disease and related neurodegenerative tauopathies. *J Med Chem*. Nov 8 2012;55(21):8979-96. doi:10.1021/jm301079z

89. Zhu Z, Chuckowree JA, Musgrove R, Dickson TC, Blizzard CA. The pathologic outcomes and efficacy of epothilone treatment following traumatic brain injury is determined by age. *Neurobiol Aging*. Sep 2020;93:85-96. doi:10.1016/j.neurobiolaging.2020.03.023

90. Ruschel J, Hellal F, Flynn KC, et al. Axonal regeneration. Systemic administration of epothilone B promotes axon regeneration after spinal cord injury. *Science*. Apr 17 2015;348(6232):347-52. doi:10.1126/science.aaa2958

91. Griffin JM, Hingorani Jai Prakash S, Bockemühl T, et al. Rehabilitation enhances epothilone-induced locomotor recovery after spinal cord injury. *Brain Commun*. 2023;5(1):fcad005. doi:10.1093/braincomms/fcad005

92. Mao L, Gao W, Chen S, et al. Epothilone B impairs functional recovery after spinal cord injury by increasing secretion of macrophage colony-stimulating factor. *Cell Death Dis*. Nov 2 2017;8(11):e3162. doi:10.1038/cddis.2017.542

93. Sandner B, Puttagunta R, Motsch M, et al. Systemic epothilone D improves hindlimb function after spinal cord contusion injury in rats. *Exp Neurol*. Aug 2018;306:250-259. doi:10.1016/j.expneurol.2018.01.018

94. Blight AR, Tuszynski MH. Clinical trials in spinal cord injury. *J Neurotrauma*. Mar-Apr 2006;23(3-4):586-93. doi:10.1089/neu.2006.23.586

95. Eidelberg E, Walden JG, Nguyen LH. Locomotor control in macaque monkeys. *Brain*. Dec 1981;104(Pt 4):647-63. doi:10.1093/brain/104.4.647-a

96. Nout YS, Rosenzweig ES, Brock JH, et al. Animal models of neurologic disorders: a nonhuman primate model of spinal cord injury. *Neurotherapeutics*. Apr 2012;9(2):380-92. doi:10.1007/s13311-012-0114-0

97. Vilensky JA, O'Connor BL. Stepping in nonhuman primates with a complete spinal cord transection: old and new data, and implications for humans. *Ann N Y Acad Sci*. Nov 16 1998;860:528-30. doi:10.1111/j.1749-6632.1998.tb09095.x

98. Noble LJ, Wrathall JR. Spinal cord contusion in the rat: morphometric analyses of alterations in the spinal cord. *Exp Neurol*. Apr 1985;88(1):135-49. doi:10.1016/0014-4886(85)90119-0

99. Taoka Y, Okajima K, Uchiba M, et al. Role of neutrophils in spinal cord injury in the rat. *Neuroscience*. Aug 1997;79(4):1177-82. doi:10.1016/s0306-4522(97)00011-0

100. Kigerl KA, McGaughy VM, Popovich PG. Comparative analysis of lesion development and intraspinal inflammation in four strains of mice following spinal contusion injury. *J Comp Neurol*. Feb 1 2006;494(4):578-94. doi:10.1002/cne.20827

101. Kjell J, Olson L. Rat models of spinal cord injury: from pathology to potential therapies. *Dis Model Mech*. Oct 1 2016;9(10):1125-1137. doi:10.1242/dmm.025833

102. Cheriyan T, Ryan DJ, Weinreb JH, et al. Spinal cord injury models: a review. *Spinal Cord*. Aug 2014;52(8):588-95. doi:10.1038/sc.2014.91

103. Joshi M, Fehlings MG. Development and characterization of a novel, graded model of clip compressive spinal cord injury in the mouse: Part 1. Clip design, behavioral outcomes, and histopathology. *J Neurotrauma*. Feb 2002;19(2):175-90. doi:10.1089/08977150252806947

104. Poon PC, Gupta D, Shoichet MS, Tator CH. Clip compression model is useful for thoracic spinal cord injuries: histologic and functional correlates. *Spine (Phila Pa 1976)*. Dec 1 2007;32(25):2853-9. doi:10.1097/BRS.0b013e31815b7e6b

105. Rhee P, Kuncir EJ, Johnson L, et al. Cervical spine injury is highly dependent on the mechanism of injury following blunt and penetrating assault. *J Trauma*. Nov 2006;61(5):1166-70. doi:10.1097/01.ta.0000188163.52226.97

106. Fawcett JW, Curt A, Steeves JD, et al. Guidelines for the conduct of clinical trials for spinal cord injury as developed by the ICCP panel: spontaneous recovery after spinal cord injury and statistical power needed for therapeutic clinical trials. *Spinal Cord*. Mar 2007;45(3):190-205. doi:10.1038/sj.sc.3102007

107. Bowes AL, Yip PK. Modulating inflammatory cell responses to spinal cord injury: all in good time. *J Neurotrauma*. Nov 1 2014;31(21):1753-66. doi:10.1089/neu.2014.3429

108. Donnelly DJ, Popovich PG. Inflammation and its role in neuroprotection, axonal regeneration and functional recovery after spinal cord injury. *Exp Neurol*. Feb 2008;209(2):378-88. doi:10.1016/j.expneurol.2007.06.009

109. Gao TY, Huang FF, Xie YY, et al. Dynamic changes in the systemic immune responses of spinal cord injury model mice. *Neural Regen Res*. Feb 2021;16(2):382-387. doi:10.4103/1673-5374.290910

110. Stirling DP, Liu S, Kubes P, Yong VW. Depletion of Ly6G/Gr-1 leukocytes after spinal cord injury in mice alters wound healing and worsens neurological outcome. *J Neurosci*. Jan 21 2009;29(3):753-64. doi:10.1523/jneurosci.4918-08.2009

111. Shechter R, London A, Varol C, et al. Infiltrating blood-derived macrophages are vital cells playing an anti-inflammatory role in recovery from spinal cord injury in mice. *PLoS Med*. Jul 2009;6(7):e1000113. doi:10.1371/journal.pmed.1000113

112. Kigerl KA, Gensel JC, Ankeny DP, Alexander JK, Donnelly DJ, Popovich PG. Identification of two distinct macrophage subsets with divergent effects causing either neurotoxicity or regeneration in the injured mouse spinal cord. *J Neurosci*. Oct 28 2009;29(43):13435-44. doi:10.1523/jneurosci.3257-09.2009

113. Cerqueira SR, Ayad NG, Lee JK. Neuroinflammation Treatment via Targeted Delivery of Nanoparticles. *Front Cell Neurosci*. 2020;14:576037. doi:10.3389/fncel.2020.576037

114. Mann AP, Scodeller P, Hussain S, et al. A peptide for targeted, systemic delivery of imaging and therapeutic compounds into acute brain injuries. *Nat Commun*. Jun 28 2016;7:11980. doi:10.1038/ncomms11980

115. Gu C, Geng X, Wu Y, et al. Engineered Macrophage Membrane-Coated Nanoparticles with Enhanced CCR2 Expression Promote Spinal Cord Injury Repair by Suppressing Neuroinflammation and Neuronal death. *Small*. Mar 2024;20(10):e2305659. doi:10.1002/smll.202305659

116. Yun X, Maximov VD, Yu J, Zhu H, Vertegel AA, Kindy MS. Nanoparticles for targeted delivery of antioxidant enzymes to the brain after cerebral ischemia and reperfusion injury. *J Cereb Blood Flow Metab*. Apr 2013;33(4):583-92. doi:10.1038/jcbfm.2012.209

117. Stirling DP, Yong VW. Dynamics of the inflammatory response after murine spinal cord injury revealed by flow cytometry. *J Neurosci Res*. Jul 2008;86(9):1944-58. doi:10.1002/jnr.21659

118. Carlson SL, Parrish ME, Springer JE, Doty K, Dossett L. Acute inflammatory response in spinal cord following impact injury. *Exp Neurol*. May 1998;151(1):77-88. doi:10.1006/exnr.1998.6785

119. Stirling DR, Swain-Bowden MJ, Lucas AM, Carpenter AE, Cimini BA, Goodman A. CellProfiler 4: improvements in speed, utility and usability. *BMC Bioinformatics*. Sep 10 2021;22(1):433. doi:10.1186/s12859-021-04344-9

120. Schindelin J, Arganda-Carreras I, Frise E, et al. Fiji: an open-source platform for biological-image analysis. *Nat Methods*. Jun 28 2012;9(7):676-82. doi:10.1038/nmeth.2019

121. Berg S, Kutra D, Kroeger T, et al. ilastik: interactive machine learning for (bio)image analysis. *Nat Methods*. Dec 2019;16(12):1226-1232. doi:10.1038/s41592-019-0582-9

122. Carlson BM, Billington L, Faulkner J. Studies on the regenerative recovery of long-term denervated muscle in rats. *Restor Neurol Neurosci*. Jan 1 1996;10(2):77-84. doi:10.3233/rnn-1996-10203

123. Rowan SL, Rygiel K, Purves-Smith FM, Solbak NM, Turnbull DM, Hepple RT. Denervation causes fiber atrophy and myosin heavy chain co-expression in senescent skeletal muscle. *PLoS One*. 2012;7(1):e29082. doi:10.1371/journal.pone.0029082

124. Spector SA. Trophic effects on the contractile and histochemical properties of rat soleus muscle. *J Neurosci*. Aug 1985;5(8):2189-96. doi:10.1523/jneurosci.05-08-02189.1985

125. Wu P, Chawla A, Spinner RJ, et al. Key changes in denervated muscles and their impact on regeneration and reinnervation. *Neural Regen Res*. Oct 15 2014;9(20):1796-809. doi:10.4103/1673-5374.143424

126. Tosolini AP, Mohan R, Morris R. Targeting the full length of the motor end plate regions in the mouse forelimb increases the uptake of fluoro-gold into corresponding spinal cord motor neurons. *Front Neurol*. 2013;4:58. doi:10.3389/fneur.2013.00058

127. Noble BT, Brennan FH, Popovich PG. The spleen as a neuroimmune interface after spinal cord injury. *J Neuroimmunol*. Aug 15 2018;321:1-11. doi:10.1016/j.jneuroim.2018.05.007

128. Milich LM, Ryan CB, Lee JK. The origin, fate, and contribution of macrophages to spinal cord injury pathology. *Acta Neuropathol*. May 2019;137(5):785-797. doi:10.1007/s00401-019-01992-3

129. Fleming JC, Norenberg MD, Ramsay DA, et al. The cellular inflammatory response in human spinal cords after injury. *Brain*. Dec 2006;129(Pt 12):3249-69. doi:10.1093/brain/awl296

130. Saito E, Kuo R, Pearson RM, et al. Designing drug-free biodegradable nanoparticles to modulate inflammatory monocytes and neutrophils for ameliorating inflammation. *J Control Release*. Apr 28 2019;300:185-196. doi:10.1016/j.jconrel.2019.02.025

131. Yin Z, Wan B, Gong G, Yin J. ROS: Executioner of regulating cell death in spinal cord injury. *Front Immunol*. 2024;15:1330678. doi:10.3389/fimmu.2024.1330678

132. Yu M, Wang Z, Wang D, Aierxi M, Ma Z, Wang Y. Oxidative stress following spinal cord injury: From molecular mechanisms to therapeutic targets. *J Neurosci Res*. Oct 2023;101(10):1538-1554. doi:10.1002/jnr.25221

133. Shi R, Kelly TM, Blight AR. Conduction block in acute and chronic spinal cord injury: different dose-response characteristics for reversal by 4-aminopyridine. *Exp Neurol*. Dec 1997;148(2):495-501. doi:10.1006/exnr.1997.6706

134. James ND, Bartus K, Grist J, Bennett DL, McMahon SB, Bradbury EJ. Conduction failure following spinal cord injury: functional and anatomical changes from acute to chronic stages. *J Neurosci*. Dec 14 2011;31(50):18543-55. doi:10.1523/jneurosci.4306-11.2011

135. Allison DJ, Ditor DS. Immune dysfunction and chronic inflammation following spinal cord injury. *Spinal Cord*. Jan 2015;53(1):14-8. doi:10.1038/sc.2014.184

136. Schwab JM, Zhang Y, Kopp MA, Brommer B, Popovich PG. The paradox of chronic neuroinflammation, systemic immune suppression, autoimmunity after traumatic chronic spinal cord injury. *Exp Neurol*. Aug 2014;258:121-129. doi:10.1016/j.expneurol.2014.04.023

137. Adams KL, Gallo V. The diversity and disparity of the glial scar. *Nat Neurosci*. Jan 2018;21(1):9-15. doi:10.1038/s41593-017-0033-9

138. Shafqat A, Albalkhi I, Magableh HM, Saleh T, Alkattan K, Yaqinuddin A. Tackling the glial scar in spinal cord regeneration: new discoveries and future directions. *Front Cell Neurosci*. 2023;17:1180825. doi:10.3389/fncel.2023.1180825

139. Xue X, Wu X, Fan Y, et al. Heterogeneous fibroblasts contribute to fibrotic scar formation after spinal cord injury in mice and monkeys. *Nat Commun*. Jul 27 2024;15(1):6321. doi:10.1038/s41467-024-50564-x

140. Fagoe ND, van Heest J, Verhaagen J. Spinal cord injury and the neuron-intrinsic regeneration-associated gene program. *Neuromolecular Med*. Dec 2014;16(4):799-813. doi:10.1007/s12017-014-8329-3

141. Kopper TJ, Zhang B, Bailey WM, Bethel KE, Gensel JC. The effects of myelin on macrophage activation are phenotypic specific via cPLA(2) in the context of spinal cord injury inflammation. *Sci Rep*. Mar 18 2021;11(1):6341. doi:10.1038/s41598-021-85863-6

142. Yao F, Luo Y, Chen Y, et al. Myelin Debris Impairs Tight Junctions and Promotes the Migration of Microvascular Endothelial Cells in the Injured Spinal Cord. *Cell Mol Neurobiol*. Mar 2023;43(2):741-756. doi:10.1007/s10571-022-01203-w

143. Geremia NM, Hryciw T, Bao F, et al. The effectiveness of the anti-CD11d treatment is reduced in rat models of spinal cord injury that produce significant levels of intraspinal hemorrhage. *Exp Neurol*. Sep 2017;295:125-134. doi:10.1016/j.expneurol.2017.06.002

144. Bradbury EJ, Carter LM. Manipulating the glial scar: chondroitinase ABC as a therapy for spinal cord injury. *Brain Res Bull*. Mar 10 2011;84(4-5):306-16. doi:10.1016/j.brainresbull.2010.06.015

145. Cafferty WB, Yang SH, Duffy PJ, Li S, Strittmatter SM. Functional axonal regeneration through astrocytic scar genetically modified to digest chondroitin sulfate proteoglycans. *J Neurosci*. Feb 28 2007;27(9):2176-85. doi:10.1523/jneurosci.5176-06.2007

146. García-Alías G, Barkhuysen S, Buckle M, Fawcett JW. Chondroitinase ABC treatment opens a window of opportunity for task-specific rehabilitation. *Nat Neurosci*. Sep 2009;12(9):1145-51. doi:10.1038/nn.2377

147. Rosenzweig ES, Salegio EA, Liang JJ, et al. Chondroitinase improves anatomical and functional outcomes after primate spinal cord injury. *Nat Neurosci*. Aug 2019;22(8):1269-1275. doi:10.1038/s41593-019-0424-1

148. Muir E, De Winter F, Verhaagen J, Fawcett J. Recent advances in the therapeutic uses of chondroitinase ABC. *Exp Neurol*. Nov 2019;321:113032. doi:10.1016/j.expneurol.2019.113032

149. Smith DR, Dumont CM, Ciciriello AJ, et al. PLG Bridge Implantation in Chronic SCI Promotes Axonal Elongation and Myelination. *ACS Biomater Sci Eng*. Dec 9 2019;5(12):6679-6690. doi:10.1021/acsbiomaterials.9b01012

150. Zhou J, Li S, Gao J, et al. Epothilone B Facilitates Peripheral Nerve Regeneration by Promoting Autophagy and Migration in Schwann Cells. *Front Cell Neurosci*. 2020;14:143. doi:10.3389/fncel.2020.00143

151. Anderson MA, Burda JE, Ren Y, et al. Astrocyte scar formation aids central nervous system axon regeneration. *Nature*. Apr 14 2016;532(7598):195-200. doi:10.1038/nature17623

152. Gu Y, Cheng X, Huang X, et al. Conditional ablation of reactive astrocytes to dissect their roles in spinal cord injury and repair. *Brain Behav Immun*. Aug 2019;80:394-405. doi:10.1016/j.bbi.2019.04.016

153. Bellver-Landete V, Bretheau F, Mailhot B, et al. Microglia are an essential component of the neuroprotective scar that forms after spinal cord injury. *Nat Commun*. Jan 31 2019;10(1):518. doi:10.1038/s41467-019-08446-0

154. Hoffmann J, Fichtner I, Lemm M, et al. Sagopilone crosses the blood-brain barrier in vivo to inhibit brain tumor growth and metastases. *Neuro Oncol*. Apr 2009;11(2):158-66. doi:10.1215/15228517-2008-072

155. Brizuela M, Blizzard CA, Chuckowree JA, et al. The microtubule-stabilizing drug Epothilone D increases axonal sprouting following transection injury in vitro. *Mol Cell Neurosci*. May 2015;66(Pt B):129-40. doi:10.1016/j.mcn.2015.02.006

156. Clark JA, Chuckowree JA, Dyer MS, Dickson TC, Blizzard CA. Epothilone D alters normal growth, viability and microtubule dependent intracellular functions of cortical neurons in vitro. *Sci Rep*. Jan 22 2020;10(1):918. doi:10.1038/s41598-020-57718-z

157. Almad A, Sahinkaya FR, McTigue DM. Oligodendrocyte fate after spinal cord injury. *Neurotherapeutics*. Apr 2011;8(2):262-73. doi:10.1007/s13311-011-0033-5

158. Sharif-Alhoseini M, Khormali M, Rezaei M, et al. Animal models of spinal cord injury: a systematic review. *Spinal Cord*. Aug 2017;55(8):714-721. doi:10.1038/sc.2016.187

159. Verstappen K, Aquarius R, Klymov A, et al. Systematic Evaluation of Spinal Cord Injury Animal Models in the Field of Biomaterials. *Tissue Eng Part B Rev*. Dec 2022;28(6):1169-1179. doi:10.1089/ten.TEB.2021.0194

160. Zhang N, Fang M, Chen H, Gou F, Ding M. Evaluation of spinal cord injury animal models. *Neural Regen Res*. Nov 15 2014;9(22):2008-12. doi:10.4103/1673-5374.143436

161. Fehlings MG, Wilson JR, Tetreault LA, et al. A Clinical Practice Guideline for the Management of Patients With Acute Spinal Cord Injury: Recommendations on the Use of Methylprednisolone Sodium Succinate. *Global Spine J*. Sep 2017;7(3 Suppl):203s-211s. doi:10.1177/2192568217703085

162. Kong X, Gao J. Macrophage polarization: a key event in the secondary phase of acute spinal cord injury. *J Cell Mol Med*. May 2017;21(5):941-954. doi:10.1111/jcmm.13034

163. Ohms M, Möller S, Laskay T. An Attempt to Polarize Human Neutrophils Toward N1 and N2 Phenotypes in vitro. *Front Immunol*. 2020;11:532. doi:10.3389/fimmu.2020.00532

164. Nguyen HX, Beck KD, Anderson AJ. Quantitative assessment of immune cells in the injured spinal cord tissue by flow cytometry: a novel use for a cell purification method. *J Vis Exp*. Apr 9 2011;(50)doi:10.3791/2698

165. Gillespie ER, Grice LF, Courtney IG, et al. Single-cell RNA sequencing reveals peripheral blood leukocyte responses to spinal cord injury in mice with humanised immune systems. *J Neuroinflammation*. Mar 1 2024;21(1):63. doi:10.1186/s12974-024-03048-0

166. Bartanusz V, Jezova D, Alajajian B, Digicaylioglu M. The blood-spinal cord barrier: morphology and clinical implications. *Ann Neurol*. Aug 2011;70(2):194-206. doi:10.1002/ana.22421

167. Jin LY, Li J, Wang KF, et al. Blood-Spinal Cord Barrier in Spinal Cord Injury: A Review. *J Neurotrauma*. May 1 2021;38(9):1203-1224. doi:10.1089/neu.2020.7413

168. Skinnider MA, Gautier M, Teo AYY, et al. Single-cell and spatial atlases of spinal cord injury in the Tabulae Paralytica. *Nature*. Jul 2024;631(8019):150-163. doi:10.1038/s41586-024-07504-y

169. Lin Y, Vreman HJ, Wong RJ, Tjoa T, Yamauchi T, Noble-Haeusslein LJ. Heme oxygenase-1 stabilizes the blood-spinal cord barrier and limits oxidative stress and white matter damage in the acutely injured murine spinal cord. *J Cereb Blood Flow Metab*. May 2007;27(5):1010-21. doi:10.1038/sj.jcbfm.9600412

170. Kimura A, Hsu M, Seldin M, Verkman AS, Scharfman HE, Binder DK. Protective role of aquaporin-4 water channels after contusion spinal cord injury. *Ann Neurol*. Jun 2010;67(6):794-801. doi:10.1002/ana.22023

171. McKenzie AL, Hall JJ, Aihara N, Fukuda K, Noble LJ. Immunolocalization of endothelin in the traumatized spinal cord: relationship to blood-spinal cord barrier breakdown. *J Neurotrauma*. Jun 1995;12(3):257-68. doi:10.1089/neu.1995.12.257

172. Winkler EA, Sengillo JD, Bell RD, Wang J, Zlokovic BV. Blood-spinal cord barrier pericyte reductions contribute to increased capillary permeability. *J Cereb Blood Flow Metab*. Oct 2012;32(10):1841-52. doi:10.1038/jcbfm.2012.113

173. Cohen DM, Patel CB, Ahobila-Vajjula P, et al. Blood-spinal cord barrier permeability in experimental spinal cord injury: dynamic contrast-enhanced MRI. *NMR Biomed*. Apr 2009;22(3):332-41. doi:10.1002/nbm.1343

174. Behzadi S, Serpooshan V, Tao W, et al. Cellular uptake of nanoparticles: journey inside the cell. *Chem Soc Rev*. Jul 17 2017;46(14):4218-4244. doi:10.1039/c6cs00636a

175. Fröhlich E. The role of surface charge in cellular uptake and cytotoxicity of medical nanoparticles. *Int J Nanomedicine*. 2012;7:5577-91. doi:10.2147/ijn.S36111

176. Foroozandeh P, Aziz AA. Insight into Cellular Uptake and Intracellular Trafficking of Nanoparticles. *Nanoscale Res Lett*. Oct 25 2018;13(1):339. doi:10.1186/s11671-018-2728-6

177. Sroga JM, Jones TB, Kigerl KA, McGaughy VM, Popovich PG. Rats and mice exhibit distinct inflammatory reactions after spinal cord injury. *J Comp Neurol*. Jul 21 2003;462(2):223-40. doi:10.1002/cne.10736

178. Byrnes KR, Fricke ST, Faden AI. Neuropathological differences between rats and mice after spinal cord injury. *J Magn Reson Imaging*. Oct 2010;32(4):836-46. doi:10.1002/jmri.22323